

Creep and consolidation of a stiff clay under saturated and unsaturated conditions

Rezania, M., Bagheri, M. & Mousavi Nezhad, M.

Author post-print (accepted) deposited by Coventry University's Repository

Original citation & hyperlink:

Rezania, M, Bagheri, M & Mousavi Nezhad, M 2019, 'Creep and consolidation of a stiff clay under saturated and unsaturated conditions' Canadian Geotechnical Journal, vol. (In-press), pp. (In-press).

<https://dx.doi.org/10.1139/cgj-2018-0398>

DOI 10.1139/cgj-2018-0398

ISSN 0008-3674

ESSN 1208-6010

Publisher: NRC Research Press (Canadian Science Publishing)

Copyright © and Moral Rights are retained by the author(s) and/ or other copyright owners. A copy can be downloaded for personal non-commercial research or study, without prior permission or charge. This item cannot be reproduced or quoted extensively from without first obtaining permission in writing from the copyright holder(s). The content must not be changed in any way or sold commercially in any format or medium without the formal permission of the copyright holders.

This document is the author's post-print version, incorporating any revisions agreed during the peer-review process. Some differences between the published version and this version may remain and you are advised to consult the published version if you wish to cite from it.

17 Abstract

18 In this paper the one-dimensional (1D) time-dependent behaviour of natural and reconstituted
19 London Clay samples under saturated and unsaturated conditions is studied. For this purpose, a
20 set of 1D consolidation tests including multi-staged loading (MSL) oedometer tests and single-
21 staged loading (SSL) long-term oedometer creep tests were carried out on saturated and
22 unsaturated specimens. Conventional oedometer cells were used for tests on saturated specimens,
23 whereas a newly designed unsaturated oedometer cell, equipped with two high-capacity
24 tensiometers (HCTs) for suction measurements, was used for unsaturated tests. The tests results
25 revealed stress- and suction-dependency of primary and secondary consolidation responses of the
26 soil samples. Furthermore, counter to formerly acknowledged suggestions of independency of the
27 slope of normal consolidation line to suction changes, it was observed that an increase in suction
28 results in a decrease of the slope of compression curve (C_c) and the creep index (C_{ae}) values, and
29 an increase in yield vertical net stress (σ_p). Moreover, the C_{ae}/C_c ratio for London Clay was found
30 to be stress- and suction-dependent, unlike the previously suggested hypotheses.

31 **Keywords:** Stiff clay, Creep, Oedometer, Suction, Unsaturated soils

32

33 **Introduction**

34 Experimental investigations have proven dependency of the mechanical behaviour of clays on
35 time effects (Li et al. 2003; Mesri 2009; Karstunen and Yin 2010; Bagheri et al. 2015; Yin and
36 Feng 2017; Rezania et al. 2017; Bagheri et al. 2019b). These effects are commonly observed as
37 post-construction deformations of geostuctures such as roads, railways, and dams. The time-
38 dependency of mechanical response is usually observed through irreversible creep deformations
39 which are typically coupled with external sources of deformations driven by, for example, repeated
40 loadings, rainfalls, flooding, and earthquakes (Oldecop and Alonso 2007). The main focus of the
41 reported works in the literature has been laid on characterisation of creep deformations in saturated
42 soft clays. This is while the shallow depth soil layers, typically studied for practical engineering
43 purposes, are usually found in partially-saturated states. Little is currently known about the
44 compression and creep response of unsaturated clays, in particular stiff clays such as London Clay
45 (LC). The reported works on creep response in unsaturated conditions are limited to observations
46 of time-dependent volume change behaviour of reservoir chalks (De Gennaro et al. 2003; De
47 Gennaro et al. 2005; Priol et al. 2007; Pereira and De Gennaro 2010), rockfills (Oldecop and
48 Alonso 2007), and reconstituted clays (Lai et al. 2010; Nazer and Tarantino 2016). Priol et al.
49 (2007) performed a set of multi-staged loading creep oedometer tests on oil-saturated, water-
50 saturated, partially-saturated, and dry Lixhe chalk (an outcrop chalk from Belgium) and reported
51 that at high pressures the creep index (C_{ae}) values increased with increase in vertical stress and
52 decreased with increase in suction (s). Similar results were reported by De Gennaro et al. (2005)
53 who evaluated the suction- and stress-dependency of creep index in MSL compression tests on
54 Estreux chalk under dry, water-saturated, and unsaturated ($s = 1.5$ MPa) conditions using a
55 suction-controlled osmotic oedometer cell. The results of unsaturated triaxial drained creep tests
56 performed on sliding zone soils of the Qianjiangping landslide (Lai et al. 2010) demonstrated that
57 an increase in matric suction results in a decrease in creep strain rate and magnitude under constant
58 net confining pressure and deviatoric stress. However, despite practical interests, generalisation of

59 these findings to various soil types, stress states, and suction ranges and coupling partial saturation
60 states and time effects is still an open topic.

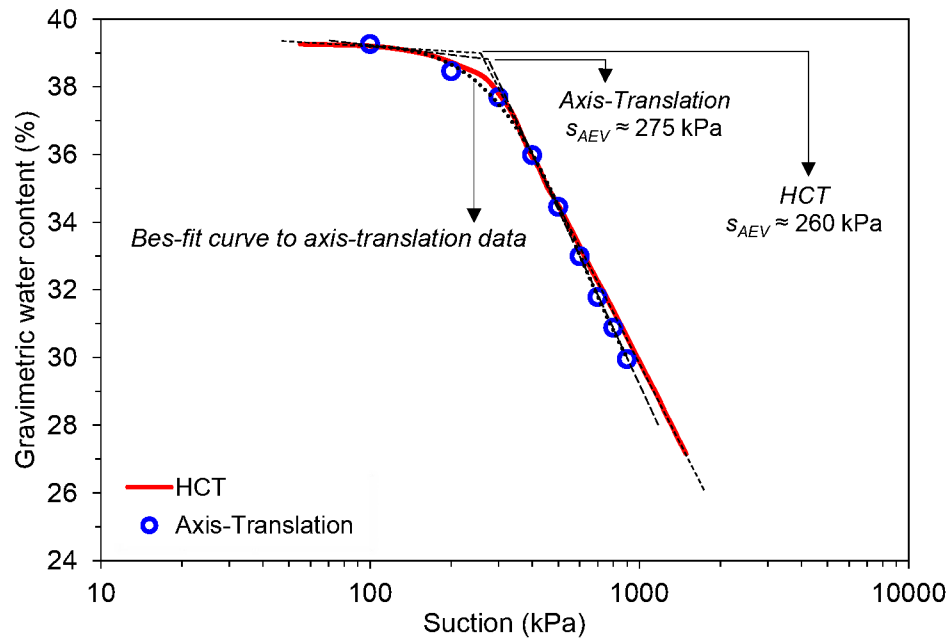
61 This paper presents the results of multi-staged loading (MSL) and single-stage loading (SSL)
62 oedometer creep tests performed on saturated and unsaturated LC specimens. Saturated tests were
63 performed on undisturbed and reconstituted specimens, whereas the unsaturated creep tests were
64 performed only on reconstituted specimens. The results of MSL tests are discussed with emphasis
65 on the effects of soil structure, suction, and vertical stress level on the compression response,
66 consolidation indices, and C_{ae}/C_c ratio. The effects of suction and vertical stress level on
67 volumetric creep strains are further discussed based on the results of SSL oedometer tests.

68 **Material and Apparatus**

69 The test material is London Clay extracted from the New Hook Farm in Isle of Sheppey in the
70 UK. Undisturbed block samples of un-weathered LC were taken at 4 m depth below non-quarried
71 ground level. The index parameters and physical properties of the natural samples are summarised
72 in Table 1. Laboratory determination of index parameters confirmed the upper bound values of
73 24% and 78% for respectively plastic limit (w_p) and liquid limit (w_L) indices. Based on the USCS
74 classification, the samples are classified as clay of high plasticity (CH).

75 The particle size distribution (PSD) curve of natural LC presents 98% particles passing through
76 the 0.063 mm sieve. The high content of fine grain inclusions results in an air-entry value (AEV)
77 of several megapascals (e.g. [Monroy et al. 2008](#)). In order to decrease the AEV, the PSD was
78 modified by including larger sized aggregates, resulting from crushing the oven-dried samples,
79 and passing through 1.18 mm sieve. The soil water retention curve (SWRC) and AEV of the
80 sample with modified PSD were measured using axis-translation and high-capacity tensiometer
81 (HCT) techniques following the procedure outlined in [Bagheri et al. \(2019a\)](#). As shown in Fig. 1,
82 the modified sample exhibited an AEV of around 260 kPa which allows for testing specimens over

83 a wider range of suctions lying on the transition (de-saturation) phase of the SWRC. It must be
 84 noted here that, although it is desired to obtain the AEV from a plot of degree of saturation versus
 85 suction, reliable values for the AEV can be also derived from the plot of water content versus
 86 suction (Fredlund 2006).



87

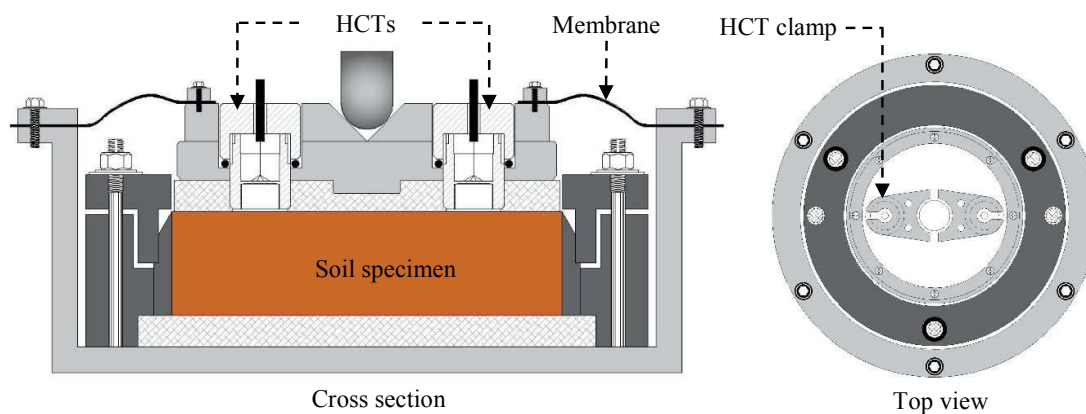
88

Fig. 1 SWRC determined for main drying path

89 Undisturbed oedometer specimens were directly cored from the block samples using a 75 mm
 90 diameter and 20 mm high oedometer ring. The inner wall of the ring was slightly lubricated with
 91 grease before preparing the specimen, in order to minimise the side friction effects on the stress–
 92 strain response. Reconstituted soil samples were prepared by mixing the soil powder, containing
 93 the large-sized aggregates, with distilled water at $1.5w_L$. The slurry was then consolidated in a 100
 94 mm diameter Perspex consolidometer under a vertical stress of 80 kPa for a duration of 5 days.
 95 The samples were then quickly unloaded to minimise swelling and water absorption. Reconstituted
 96 saturated specimens were cored from the obtained cylindrical soil cakes. Unsaturated specimens
 97 were cored from smaller subsamples air-dried at room temperature to pre-specified water contents
 98 and stored in air-tight containers for a duration of one week to attain moisture equilibrium.
 99 Selection of the initial water contents (w_0) of the specimens was based on the information obtained

100 from the developed SWRC for reconstituted samples and to examine compressibility of specimens
 101 with a wide range of suctions on the transition effect zone (partially saturated zone) of the main
 102 drying curve.

103 Saturated tests were carried out in conventional oedometer cells, whereas unsaturated tests were
 104 carried out in suction-monitored oedometer cells equipped with two high-capacity tensiometers
 105 (HCTs) for monitoring suction evolutions (Bagheri et al. 2018). The special design of the
 106 oedometer loading cap allows for replacement of a cavitated HCT without any disturbance to the
 107 specimen and interruption in measurement of deformations. A schematic view of the unsaturated
 108 oedometer cell is provided in Fig. 2.



110 **Fig. 2.** Schematic diagram of the unsaturated oedometer cell

111 **Experimental Program**

112 MSL oedometer tests with 24 hour loading periods were performed on intact, reconstituted, and
 113 low-quality undisturbed (LQU) specimens. Considering the fissured nature of the LC, significant
 114 attention was given during the preparation of intact specimens. Where the specimen preparation
 115 process involved minor visible damage to the soil structure, the prepared specimen was marked as
 116 LQU. Prior to the start of the tests, the w_0 and the specimen dimensions were measured for
 117 saturated MSL tests. The specimen was then set in the conventional oedometer cell and vertical
 118 load was applied step-wise to the submerged specimen during each 24 hours loading step.

119 Typically, for conventional oedometer tests, vertical load is doubled at each stage of loading. This
120 can, however, cause significant unfavourable disturbance to the structural properties of the test
121 specimen especially at high stress levels. In order to reduce such effects, in addition to the doubling
122 vertical stress method, other loading patterns, as shown in Table 2, were also considered. By the
123 end of loading to the desired stress levels, the specimens were unloaded step-wise in order to
124 evaluate the swelling response. Each unloading stage was kept for 24 hours to ensure complete
125 swelling and that most of the generated suction was released. The compression curves were finally
126 obtained based on the final settlement values. For unsaturated MSL tests, prior to each experiment,
127 the HCTs were saturated and preconditioned following the procedure explained by [Bagheri et al.](#)
128 [\(2018\)](#). In order to ensure ultimate contact between the specimen and the HCTs, the ceramic disks
129 of the tensiometers were covered with soil paste, and a small vertical stress was also applied to the
130 specimen. The average suction recorded by the two HCTs, used to monitor suction changes, at the
131 start of loading was considered as the initial suction (s_0) of the specimen. In all experiments, the
132 pressure difference recorded by the two HCTs did not exceed 5 kPa. The HCTs were also
133 periodically calibrated in order to account for any possible changes in their performance. For
134 specimens with s_0 values beyond the capacity of the HCTs, the corresponding s_0 values were
135 estimated from the curve fitting of the experimental SWRC using [Fredlung and Xing \(1994\)](#)
136 equation. Table 2 presents the details of MSL tests.

137 SSL tests were carried out only on reconstituted specimens in order to avoid the complexities
138 associated with coupled effects of suction and soil structure. Unlike conventional incremental
139 loading tests, the test pressure was applied directly in a single loading stage in order to remove the
140 possible effects of loading and creep history on the measured creep strains. Moreover, in order to
141 avoid the problems associated with sudden loading, the applied pressure was ramped up to the
142 desired vertical stress level at a constant rate of 8-10 kPa per hour. The applied pressure was
143 sustained for a period of 19 to 94 days. The values of the maximum applied vertical stresses (σ_{vm})
144 were chosen so that they were higher than the preconsolidation pressure of the samples so that it

145 was possible to investigate the creep response in the normal consolidation state. Unsaturated tests
 146 were conducted on specimens having initial suction states on the main drying curve of the SWRC
 147 in order to eliminate the complexity associated with volumetric deformation due to wetting
 148 (wetting-induced deformations or collapse in wetting), and therefore observe the effect of suction
 149 on mechanically induced creep deformations. Details of the carried out experiments are
 150 summarised in Table 3.

151 **Results**

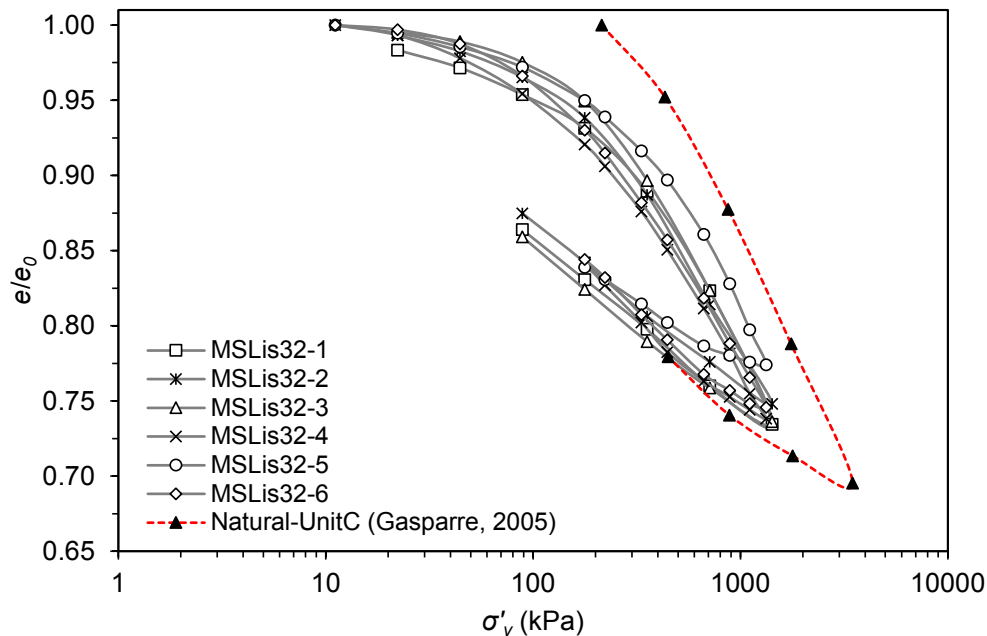
152 The compression index (C_c), swelling index (C_s), and reloading index (C_r) values were calculated
 153 as the slope of respectively the normal compression line (NCL), the swelling (unloading) line, and
 154 the reloading line of the compression curve plotted in $e - \log \sigma'_v$ space, where e is void ratio and
 155 σ'_v is vertical effective stress. As suggested by [Mataic et al. \(2016\)](#), the creep index (C_{ae}) was
 156 defined as the slope of the plot of void ratio versus logarithm of time (t) from the time period of
 157 6–24 hours for each load increment. The decrease in void ratio during this time scale represents
 158 the creep phase as the end of primary consolidation (EOP) was found to be within the first 5–6
 159 hours of each loading increment. The experimental results of unsaturated oedometer tests can be
 160 evaluated based on the generalised vertical effective stress relationship;

$$(1) \quad \sigma'_v = \sigma_{vnet} + S_r s$$

161 where S_r is the degree of saturation, s is soil suction, and $\sigma_{vnet} = \sigma_v - u_a$ is the net normal stress
 162 defined as the difference of vertical total stress (σ_v) and pore-air pressure (u_a). Estimation of S_r
 163 requires the information of the water content of the specimen during the test. However, as the
 164 suction-monitored oedometer cell does not allow for measurement of the specimens' water
 165 content, the experimental results of unsaturated oedometer tests were evaluated based on the σ_{vnet} ,
 166 and since the tests were carried out at the atmospheric air pressure, $\sigma_{vnet} = \sigma_v$.

167 ***Evaluation of Compressibility in MSL Tests***

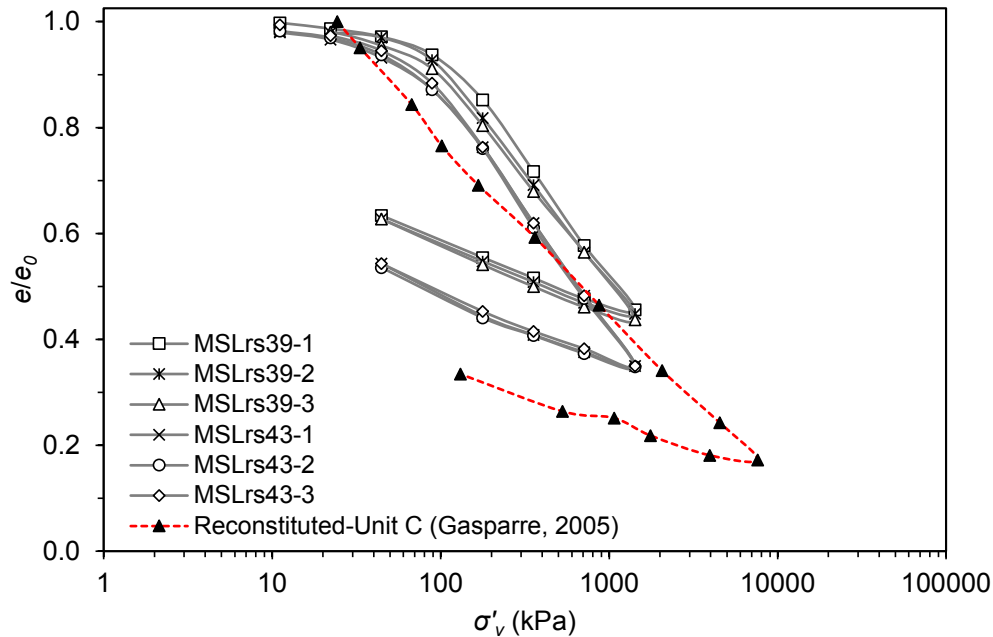
168 A comparison of the normalised compression curves for Sheppey LC and the natural LC from
 169 Unit C (block sample retrieved from 5–10 m depth) of the Heathrow Terminal 5 site (T5)
 170 (Gasparre 2005) is shown in Fig. 3. The curves exhibited very similar characteristics with almost
 171 equal compression and swelling indices. The specimen from T5, however, is less compressible
 172 than the Sheppey specimen, mainly due to its lower plasticity index ($I_p = 37\%$) and initial water
 173 content ($w_0 = 24\%$). Moreover, the change in loading pattern, which was aimed at reducing the
 174 effects of sudden loading and subsequent damages to the soil structure, did not have a notable
 175 influence on the obtained compression curves. The only exception was the MSLis32-5 curve
 176 which was slightly shifted to the right, and exhibited lower compressibility which could be due to
 177 a lower S_r of the specimen at the start of the test. Furthermore, the highly structured nature of the
 178 specimens resulted in high C_s values. Similar observations were also reported by Gasparre (2005)
 179 for LC samples retrieved from T5. Average C_c and C_s values of respectively 0.218 and 0.096 were
 180 obtained from the compression tests on intact specimens having an average initial void ratio of e_0
 181 $= 0.85$ and initial water content of $w_0 = 32\%$.



182

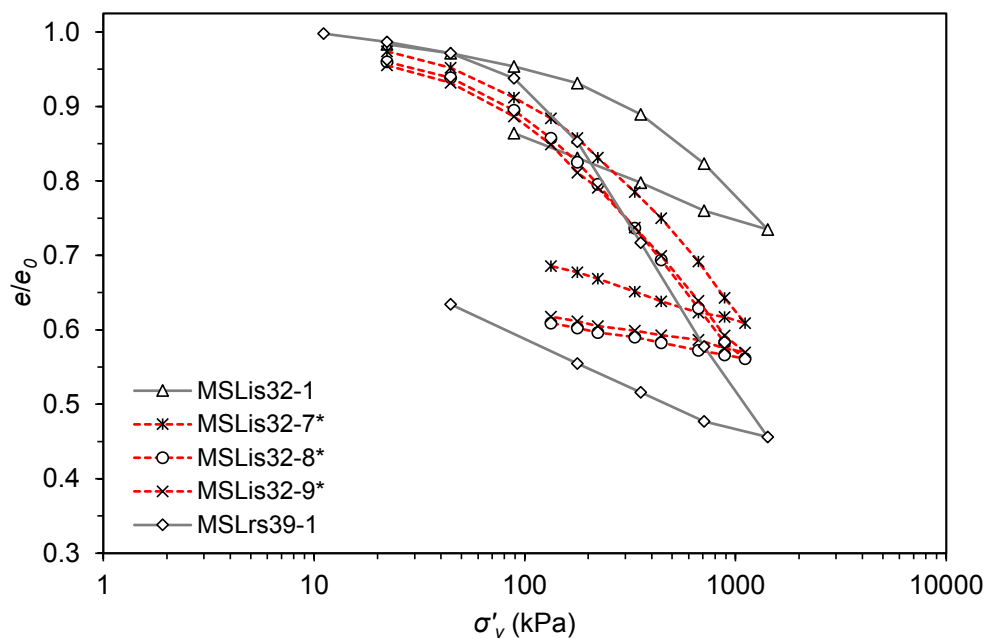
183 **Fig. 3.** Comparison of the compression curves for intact Sheppey LC and natural LC from Unit C of
 184 Heathrow T5 site

185 Fig. 4 presents the results of MSL compression tests carried out on reconstituted specimens. It is
 186 seen that with an increase of w_0 , the compressibility of the specimens is increased. Average C_c and
 187 C_s values of respectively 0.383 and 0.125 were obtained from the compression tests on
 188 reconstituted specimens having an average initial void ratio of 0.93 and initial water content of
 189 39%. For specimens with $w_0 = 43\%$, the average C_c and C_s values of respectively 0.408 and 0.133
 190 were obtained. Similar C_c values of 0.41 to 0.51 were reported by [Sorensen \(2006\)](#) from isotropic
 191 compression and oedometer tests on reconstituted LC from T5. Similar to intact specimens, the
 192 reconstituted compression curves of Sheppey and T5 LC were also compared. The reconstituted
 193 Sheppey specimen exhibits less compressibility in comparison with the reconstituted T5 specimen.
 194 This behaviour could be attributed to the modified PSD of the reconstituted Sheppey specimens
 195 and the presence of sand-sized aggregates that resulted in an increased resistance against
 196 compression.



197 **Fig. 4.** Comparison of the compression curves for reconstituted Sheppey LC and natural LC from Unit C
 198 of Heathrow T5 site
 199

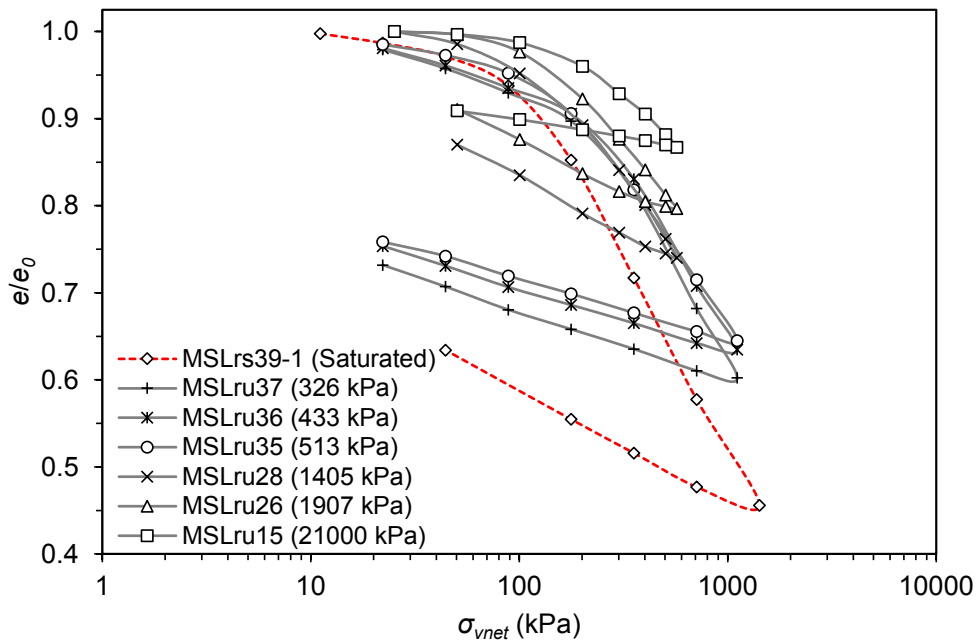
200 To further investigate the effect of soil structure on the compressibility of Sheppey LC, a set of
 201 three MSL oedometer tests were carried out on LQU specimens. A comparison of compression
 202 curves for intact, reconstituted, and LQU specimens is shown in Fig. 5. The compression curve of
 203 the LQU specimen with partly destroyed structure lies in between the compression curves of intact
 204 and reconstituted specimens. The curve is more similar to the reconstituted compression curve,
 205 highlighting the greater influence of soil structure than the initial water content on the
 206 compressibility of stiff LC.



207

208 **Fig. 5.** Comparison of the compression curves for saturated intact, reconstituted, and LQU specimens

209 Fig. 6 presents the normalised compression curves for unsaturated reconstituted specimens. As it
 210 can be seen, suction influences the shape and location of the compression curves. Increase in
 211 suction level results in a decrease in overall compressibility of the specimens. Furthermore,
 212 increase in suction results in an increase in yield vertical net stress (σ_p), a phenomenon known as
 213 suction hardening (Wheeler and Sivakumar, 1995). The obtained data allows for defining the locus
 214 of the yield points in suction-net mean stress plane known as Loading-Collapse yield curve in
 215 Barcelona Basic Model (BBM) proposed by Alonso et al. (1990).



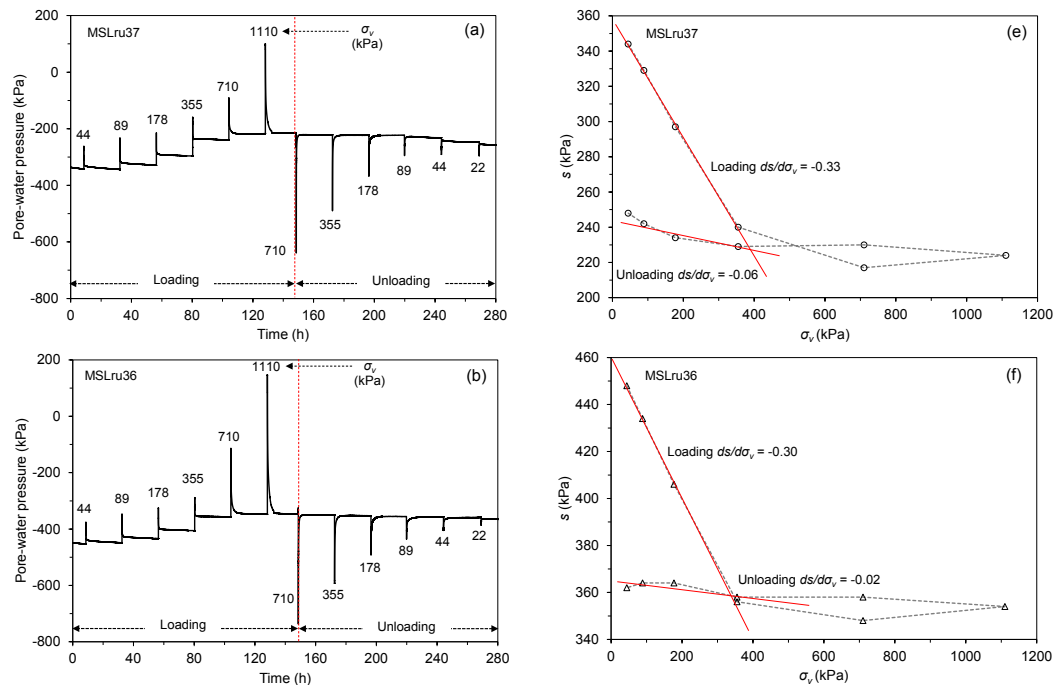
216

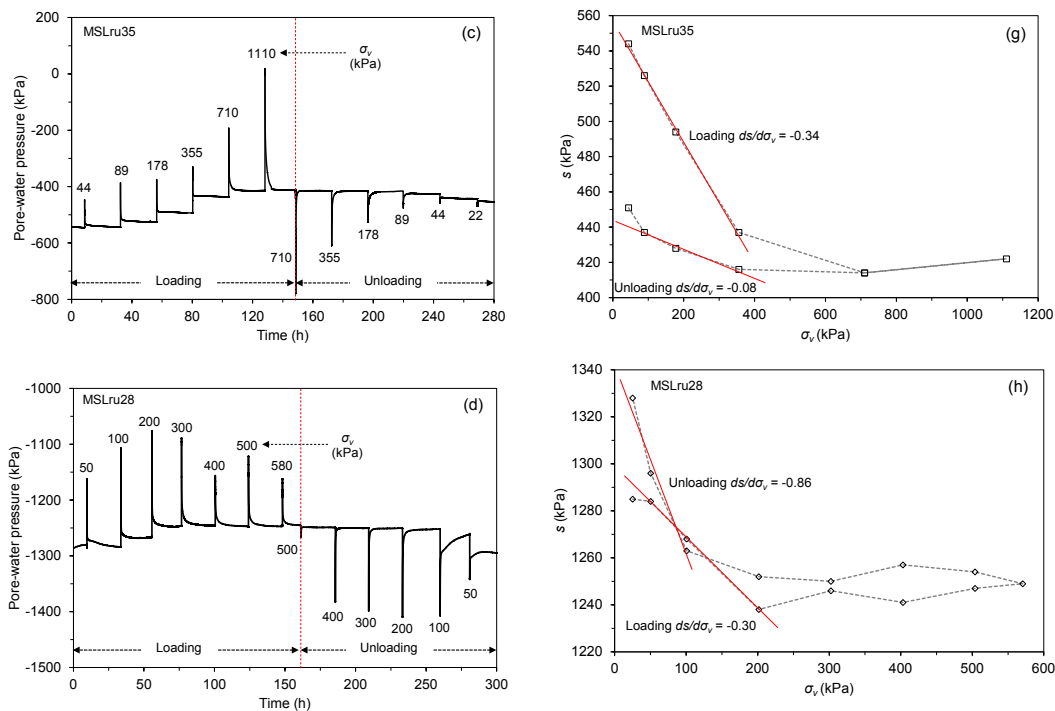
217

Fig. 6. Compression curves for unsaturated reconstituted specimens

218 Fig. 7 presents the variation of pore-water pressure (u_w) during loading and unloading stages for
 219 specimens MSLru37, MSLru36, MSLru35 and MSLru28. Figs. 7(a) to 7(d) show an
 220 instantaneous increase in u_w (decrease in suction) followed by a gradual pressure equalisation at
 221 each loading stage. Moreover, for all loading stages, a suction state was preserved within the
 222 specimens, confirming that no water had been expelled, and hence, the condition of constant water
 223 content was recognised throughout the experiments. Similarly, instantaneous decrease in u_w
 224 (increase in suction) followed by a pressure stabilisation was observed at each unloading stage.
 225 Unlike the assumption of pore-fluid incompressibility in saturated consolidation theory, the pore-
 226 fluid, being formed of gas (typically air) and liquid (typically water), is considered compressible
 227 during consolidation of unsaturated clays. Therefore, during the course of compression, with a
 228 decrease in air volume, the S_r is increased, this is mainly due to the reduction in void ratio of the
 229 specimen. The decrease in suction observed at the end of the unsaturated MSL tests can be,
 230 therefore, explained by the increase in S_r of the specimen.

231 Figs. 7(e) to 7(h) present the variation of suction with vertical stress changes ($ds/d\sigma$), once
 232 equilibrium has been reached. As it can be seen on the graphs, suction is decreased during loading
 233 and then increased by unloading. For vertical stresses up to 400 kPa (200 kPa for MSLru28), a
 234 linear relationship between changes in suction and applied vertical stress was observed. Variation
 235 of suction with vertical stresses higher than 400 kPa (200 kPa for MSLru28) appears to be almost
 236 constant during both loading and unloading stages. The slopes obtained during loading were very
 237 close and varied between -0.30 and -0.34. Except for the MSLru28 specimen, the slopes obtained
 238 during unloading were also close and varied between -0.02 and -0.08. MSLru28 exhibited a higher
 239 slope in unloading (-0.86) than loading (-0.30). For natural clays, the slopes obtained during the
 240 unloading stage can be used for estimation of suction changes during sampling and release of
 241 stresses (Delage et al. 2007). Although the experiments were performed on reconstituted samples,
 242 the obtained results clearly confirmed the importance of suction and suction release, in particular
 243 in stiff clays such as LC, even though it appears that suction changes during unloading for
 244 specimens with low initial suctions ($< \sim 500$ kPa) is not significant.





245 **Fig. 7.** Monitoring suction changes during step loading oedometer tests

246 Further inspection of Figs. 7(a) to 7(d) reveals a slight increase in equalised suction at the early
 247 stages of loading (e.g. at $\sigma_v = 89$ kPa) for MSLru37, MSLru36, and MSLru35 specimens. A
 248 possible reason for such observation is that under constant water content conditions, the change in
 249 pore-water pressure (Δu) is expressed as;

$$(2) \quad \Delta u = B \times \Delta \sigma_v + \Delta u_d$$

250 Where B is the Skempton B value ($\Delta u / \Delta \sigma_v$) and Δu_d is the excess pore-water pressure accounted
 251 for a possible dilation within the aggregates. This dilation component (Δu_d) would be negative,
 252 therefore it may subdue the overall increase in Δu caused by $\Delta \sigma_v$. Therefore, it may be expected
 253 to see an increase in suction and hence, reduction in the overall B value at the early stages of
 254 compression under undrained conditions. Evolution of B value with vertical net stress during the
 255 loading and unloading stages is shown in Fig. 8. The fact that the B value is notably high at the
 256 early stages of loading might be due the high water content of the soil paste placed on the tip of
 257 HCT to ensure intimate contact between the porous filter and surrounding soil.

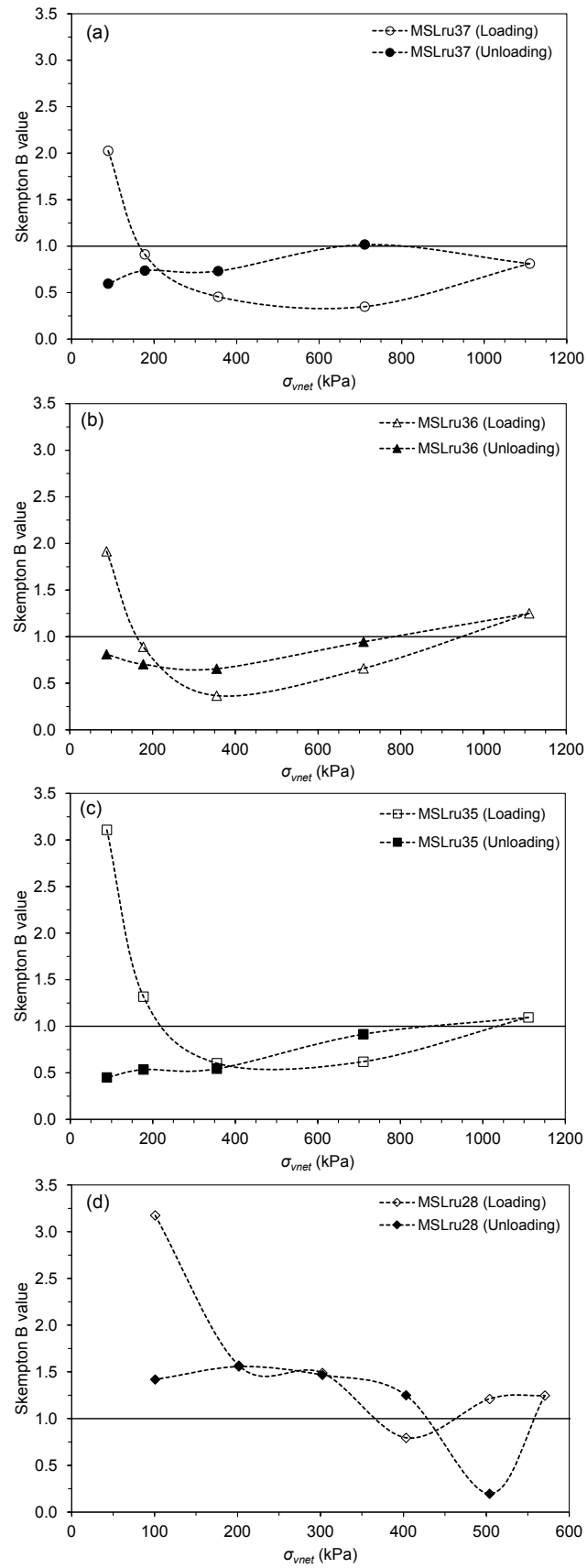
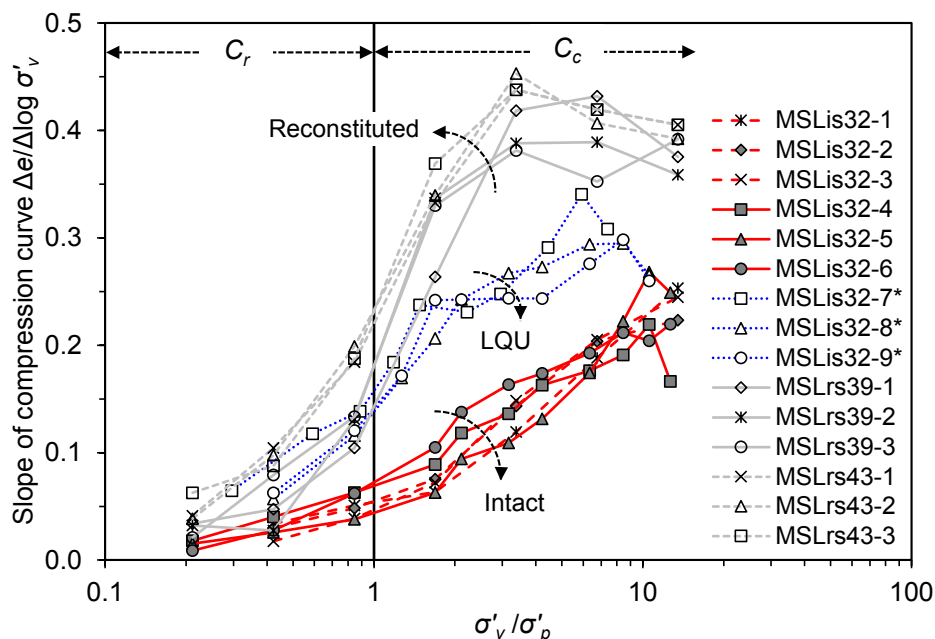


Fig. 8. Evolution of Skempton B value with vertical net stress

259 ***Stress-Dependent Response in MSL Tests***

260 Compressibility of intact and reconstituted clays can be evaluated from the variation of the slope
 261 of compression curve with vertical effective stress (σ'_v). The slope of compression curve (m_c) at
 262 each loading increment is calculated as $\Delta e / \Delta \log \sigma'_v$. The saturated yield vertical net stress (σ'_p)
 263 was determined as the intersection of the best fitted lines to the pseudo-elastic and plastic sections
 264 of the compression curve. For $\sigma'_v < \sigma'_p$, the calculated values represent the slope of the reloading
 265 line (i.e. C_r), and for $\sigma'_v > \sigma'_p$, the calculated values represent the slope of normal compression line
 266 (i.e. C_c). Fig. 9 presents the relationship between m_c and normalised stress σ'_v / σ'_p for saturated
 267 intact, reconstituted, and LQU specimens. As it can be seen, change in the loading pattern (dotted
 268 lines) does not have a significant influence on the C_r and C_c values for intact specimens. Prior to
 269 the yield stress, the C_r values increase slightly. Following σ'_p , the values of C_c increase gradually
 270 until reaching a peak value around (8-10) σ'_p , after which, a gradual decrease in compressibility is
 271 observed. Unlike soft clays that exhibit a sudden increase of C_c in post yield region due to
 272 structural collapse (see for example [Mataic et al. 2016](#)), the process of destructuration in stiff LC
 273 appears to be continuous and follows an almost linear trend until reaching the peak value. In soft
 274 clays the peak value falls in a range of (2-3) σ'_p (e.g. [Karstunen and Yin 2010](#); [Mataic et al. 2016](#)),
 275 whereas for stiff LC this range is observed to extend to (8-10) σ'_p (see Fig. 9). Similar to intact
 276 specimens, the slope of reloading line for reconstituted specimens increases slightly prior to σ'_p .
 277 Increase in slope of reloading line for specimens with $w_0 = 43\%$ is reasonably higher than the
 278 specimens with $w_0 = 39\%$ given the higher water content that results in higher compressibility.
 279 The slope of compression curve in normal consolidation (NC) region increases dramatically to a
 280 peak value at stress levels between (3-4) σ'_p , at which it starts to decrease slowly. In soft clays,
 281 higher m_c values for intact specimens is typically observed in comparison with the reconstituted
 282 specimens, mainly due to the destructuration phenomenon that results in dramatic increase of C_c
 283 values in post yield region. However, as explained earlier, in stiff LC, degradation of inter-particle
 284 bonds (destructuration) does not occur suddenly and typically takes place gradually with increase

285 in stress level. In overconsolidated (OC) region, the C_r values for LQU specimens increase at the
 286 same rate as the reconstituted specimens. However, in post yield region, the rate of increase in C_c
 287 for LQU specimens is lower than that of reconstituted specimens, this is in part, due to the lower
 288 w_0 and the presence of inter-particle bonds that result in reduction of compressibility. The
 289 maximum value of C_c for LQU specimens occurs in a range of (6-8) σ'_p .



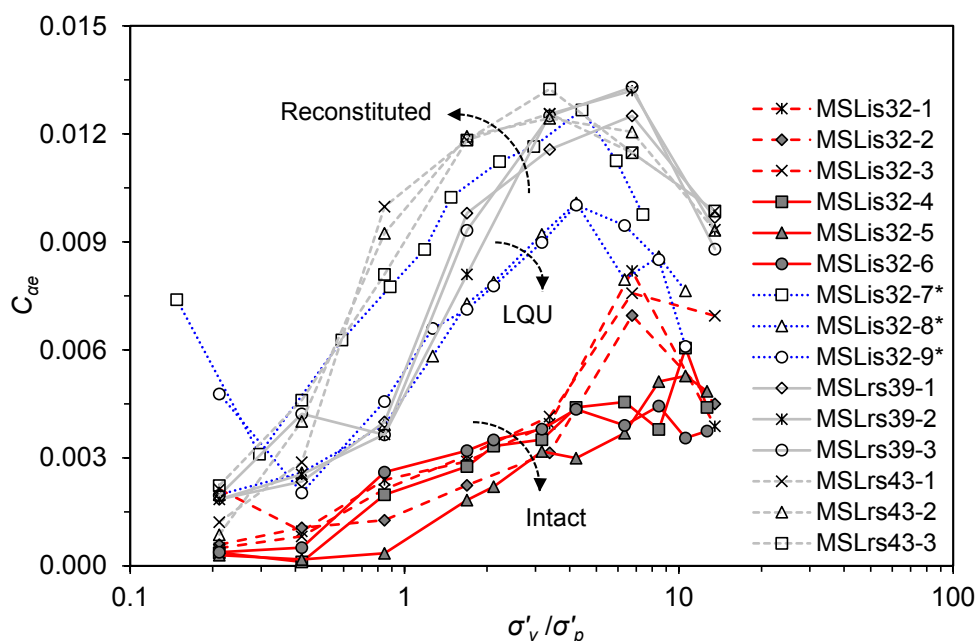
290

291 **Fig. 9.** Stress-dependency of the slope of compression curve for saturated intact, reconstituted, and LQU
 292 specimens

293 Fig. 10 presents variation of the C_{ae} with normalised stress σ'_v/σ'_p for intact, reconstituted, and
 294 LQU specimens. It is observed that for doubling vertical stress method (dotted lines), C_{ae} increases
 295 gradually with stress level up to (3-4) σ'_p , at which it starts to increase dramatically to a peak value
 296 at stress levels in a range of (6-7) σ'_p . This behaviour can be attributed to the structural damage to
 297 the specimen during sudden loading at high stress levels. After the peak value, C_{ae} decreases
 298 dramatically. For specimens that the vertical stresses were applied in an unconventional way
 299 (continuous lines) following the pattern described in Table 2, it is observed that C_{ae} increases
 300 gradually with stress level up to (8-11) σ'_p , at which it starts to decrease. This unconventional

301 loading method, therefore, appears to produce more reliable results although it involves more
302 loading stages and hence, requires more time to complete. The maximum value of C_{ae} falls
303 approximately in the range of 0.007 – 0.008 and 0.005 – 0.006 respectively for conventionally and
304 unconventionally loaded intact specimens. For reconstituted specimens with $w_0 = 39\%$, C_{ae}
305 increases slowly at stress levels prior to σ'_p . For stresses beyond yield stress, C_{ae} increases at a
306 higher rate until reaching a peak value at stress levels in a range of (6-7) σ'_p at which it starts to
307 decrease. For specimens with higher initial water content ($w_0 = 43\%$), variation of C_{ae} with
308 normalised stress is slightly different, with C_{ae} increasing dramatically in OC region and then
309 increasing gradually in NC region to a peak value at stress levels in a range of (3-4) σ'_p where a
310 gradual reduction of C_{ae} values is observed. The maximum value of C_{ae} falls approximately in the
311 range of 0.012 – 0.013 for all tested reconstituted specimens. This range is comparable with the
312 average value of $C_{ae} = 0.016$ reported by [Sorensen \(2006\)](#) for reconstituted T5 LC.

313 Unlike natural soft clays which typically exhibit higher creep than their corresponding
314 reconstituted specimens, stiff LC exhibits significantly less creep in comparison with the
315 corresponding reconstituted specimens. This, on the one hand, can be attributed to the more
316 compact nature of stiff clays (low initial void ratio) that results in reduced particles freedom for
317 rearrangement under sustained σ'_v , and on the other hand, to the low w_0 of the intact specimens
318 and presence of localised unsaturated pockets with sustainable water menisci developed at inter-
319 particle contacts preventing orientation and rearrangement of particles into a more packed state.
320 In soft clays, the C_{ae} values for intact specimens essentially converge with intrinsic C_{ae} of the
321 reconstituted specimens at high stress levels associated with the completely destroyed inter-
322 particle bonds and rearranged fabric ([Mataic et al. 2016](#)). Indeed, much higher stress levels are
323 required to observe such behaviour for stiff clays. For LQU specimens, it is observed that C_{ae}
324 increases gradually with stress level up to (4-5) σ'_p , at which it starts to decrease. The response of
325 LQU specimens is more similar to that of reconstituted ones, highlighting the effect of soil
326 structure on creep strains.



327

328

Fig. 10. Stress-dependency of C_{ae} for intact, reconstituted, and LQU specimens

329 The ratio of $\alpha = C_{ae}/C_c$ in clays has been the subject of numerous studies in the past. Although
 330 early researchers such as [Mesri and Godlewski \(1977\)](#) and [Mesri and Castro \(1987\)](#) proposed
 331 constant values for α , recent experimental studies (e.g. [Yin et al. 2011](#); [Mataic et al. 2016](#)) have
 332 demonstrated stress-dependency of α for soft clays. In order to examine the applicability of either
 333 of these two hypotheses for stiff Sheppey LC, the ratio α was investigated. Fig. 11 presents
 334 variation of C_{ae}/m_c ratio with normalised stress σ'_v/σ'_p for saturated intact, reconstituted, and LQU
 335 specimens. Unlike natural soft clays that exhibit a sudden increase to a peak value in post yield
 336 region due to destructuration phenomenon ([Mesri and Castro 1987](#); [Karstunen and Yin 2010](#);
 337 [Mataic et al. 2016](#)), variation of C_{ae}/m_c ratio with normalised stress for intact specimens does not
 338 present such trends. At lower stress levels (i.e. OC region), the C_{ae}/C_r ratio is considerably
 339 scattered. In NC region, the C_{ae}/C_c ratio decreases gradually with stress level. The values of α fall
 340 approximately in a range of 0.015 – 0.045. Moreover, the values of α for conventionally loaded
 341 specimens are generally greater than those of unconventionally loaded specimens (dotted lines).
 342 The less scattered values of α for unconventionally loaded specimens in post yield region can
 343 further approve the suitability of this loading method for investigating interrelation of compression

344 and creep indices in stiff clays. Similar to intact specimens, the C_{ae}/C_r ratio for reconstituted
345 specimens is considerably scattered at lower stress levels (i.e. OC region). However, in NC region,
346 the C_{ae}/C_c values are less scattered and decrease gradually to finally converge at the constant
347 average value of 0.024. Moreover, the values of α in post yield region are in general smaller for
348 intact specimens than reconstituted ones given lower C_c and C_{ae} values observed for intact
349 specimens (see Figs. 9 and 10). In soft clays, the C_{ae}/C_c values essentially converge at a constant
350 value corresponding to that of the reconstituted specimens. This is justified based on the principle
351 that at high stress levels, all inter-particle bonds are destroyed and the post yield compression
352 curve of a natural clay merges with the intrinsic compression line (ICL) associated with the
353 corresponding reconstituted specimen. In soft clays, convergence of C_{ae}/C_c values for intact and
354 reconstituted specimens may occur at stress levels in a range of (10-20) σ'_p due to the soft nature
355 and high degree of destructuration in these materials. However, a much higher stress level may be
356 required for degradation of inter-particle bonds in stiff clays such as LC. Applying such high
357 stresses may not be typically possible using the conventional dead-weight loading method in
358 oedometer apparatuses. Inspection of the results for LQU specimens reveals that, except for the
359 MSLis32-7* specimen, the ratio of α for LQU specimens exhibits a peak value at stress levels in
360 a range of (4-5) σ'_p , at which it starts to decrease towards the values of α ratio of the reconstituted
361 specimens. In conclusion, it is clear that the C_{ae}/C_c ratio is stress-dependent and varies with the
362 effective stresses. Therefore, the hypothesis of constant C_{ae}/C_c ratio is not applicable for the tested
363 material.

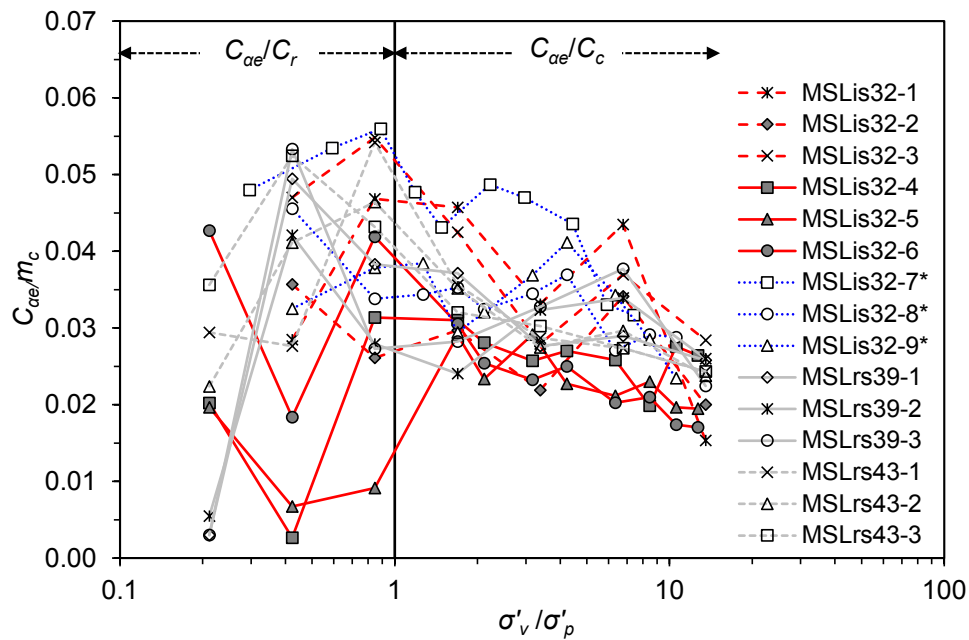


Fig. 11. Stress-dependency of C_{ae}/C_c for intact, reconstituted, and LQU specimens

364

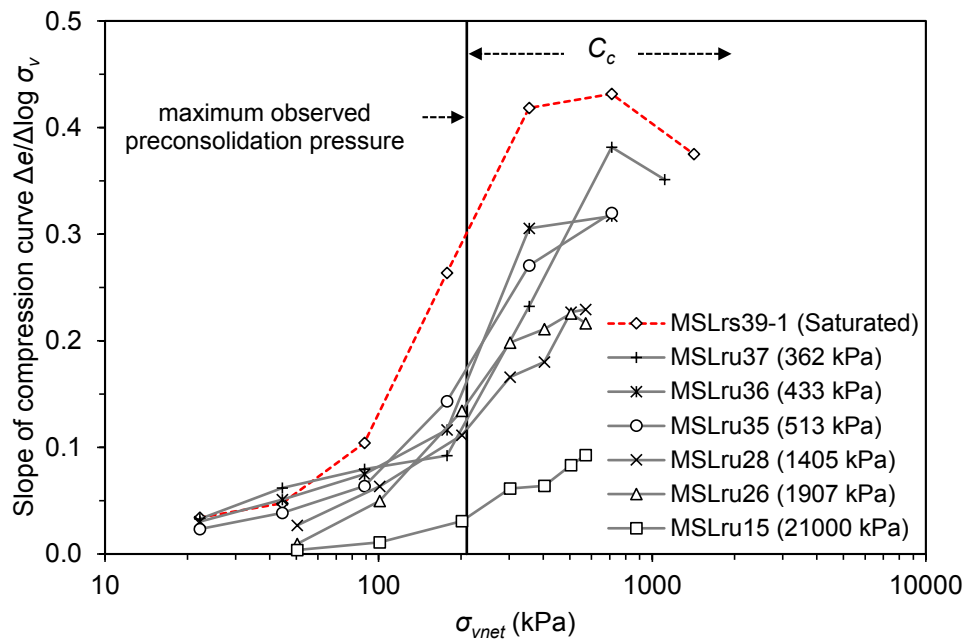
365

366

367 *Suction-Dependent Response in MSL Tests*

368 Fig. 12 presents the relationship between the slope of unsaturated compression curve ($m'_c =$
 369 $\Delta e/\Delta \log \sigma_{vnet}$) and vertical net stress (σ_{vnet}) for unsaturated reconstituted specimens. Similar to
 370 saturated reconstituted specimens (see Fig. 9), the slope of compression curves, calculated for each
 371 load increment, exhibits stress-dependency and increases with increase in σ_{vnet} . However, unlike
 372 the saturated specimens, a peak value, after which the m'_c is decreased, is not apparent. Moreover,
 373 it is clearly shown that increase in suction results in decrease of the m'_c values. To further
 374 investigate this phenomenon, the values of C_s and C_c for each test were plotted against the initial
 375 suction of the specimen (Fig. 13). It is clearly observed that the C_c values decrease with increase
 376 in suction. The C_s values also decrease with increase of suction and follow an approximately linear
 377 trend. The latter observation contradicts with the statement of [Sivakumar \(1993\)](#) that the gradient
 378 of swelling lines are almost independent of suction level. The former observation also contradicts
 379 with the results of suction-controlled oedometer tests on compacted LC, performed by [Monroy et](#)
 380 [al. \(2008\)](#), who reported an increase in C_c values with increase in soil suction. The reason behind
 381 such contradiction can be attributed to the sample preparation method and the initial conditions of

382 the test specimens. Monroy et al. (2008) prepared the samples by static compaction to an initial
 383 suction of 1000 kPa, and then decreased the suction by hydrating the samples to different
 384 equilibrium suctions (zero, 120, and 405 kPa). Therefore, the observed differences in
 385 compressibility responses can be explained, in one hand, by the differences in mechanical response
 386 of compacted and reconstituted samples, and in other hand, by the initial hydraulic states of the
 387 two samples positioned respectively on the main drying (reconstituted) and main wetting
 388 (compacted) curves of the SWRC.

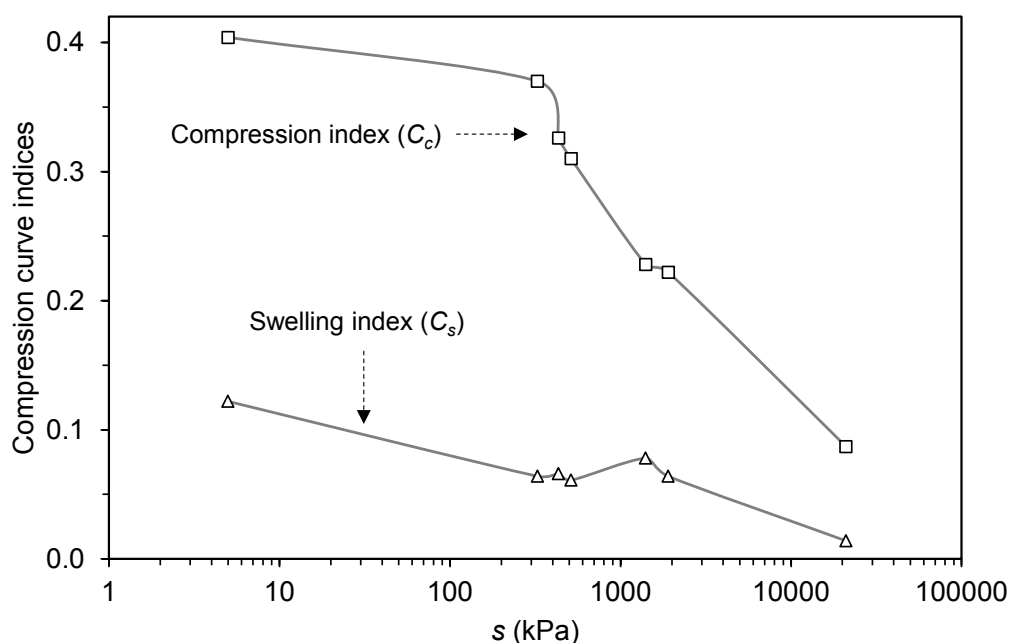


389

390 **Fig. 12.** Suction- and stress-dependency of the slope of compression curve for unsaturated reconstituted

391

specimens



392

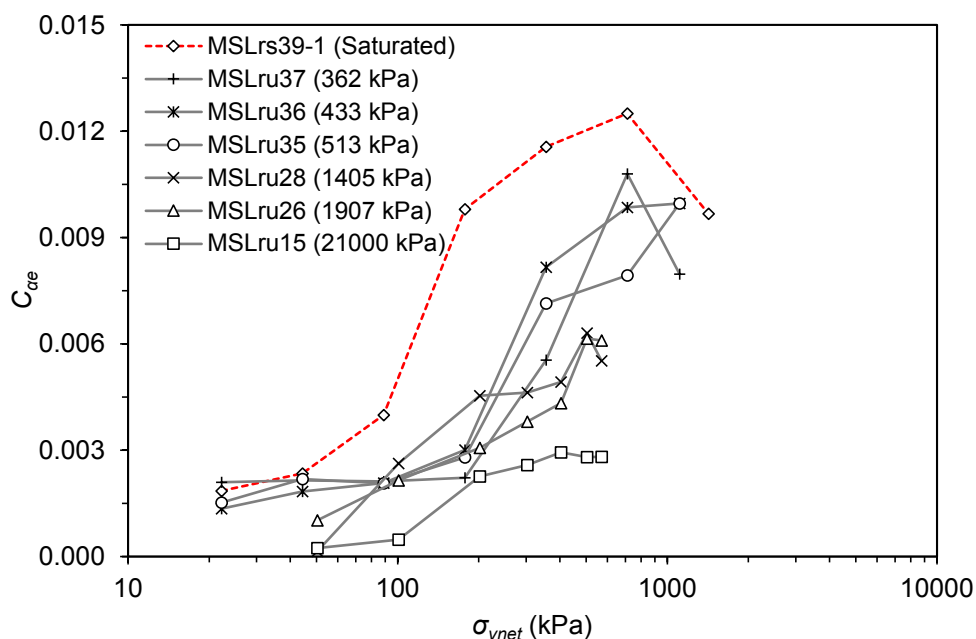
393

Fig. 13. Variation of C_c and C_s with suction for unsaturated reconstituted specimens

394 The compression index as a function of suction has been the subject of a long-term dispute among
 395 the researchers. Different approaches, as discussed in [Zhou et al. \(2012\)](#), have been proposed to
 396 overcome the problems associated with assuming C_c as a function of suction. Among which, the
 397 assumption of C_c as a function of S_r appears to be a more logical approach which also produces a
 398 better match to the experimental data when used in constitutive models ([Zhou et al. 2012](#)). This
 399 approach implies that C_c increases with increase in S_r . In other words, it is possible to saturate an
 400 unsaturated soil by compressing it under constant suction. In fact, in constant suction compression,
 401 increase in S_r as a result of reduction in void ratio, can increase the compressibility of the soil due
 402 to the stress-induced collapse of macro-pores ([Zhou et al. 2012](#)). Based on this approach, increase
 403 of C_c is small at low stresses, and becomes larger at intermediate stress levels until finally equalises
 404 the C_c value corresponding to the saturated condition. This behaviour is clearly shown in Fig. 12.
 405 The only difference is that the C_c values of unsaturated specimens do not essentially converge with
 406 the values of their saturated condition. Higher applied total stresses might be required to observe
 407 such convergences. Moreover, as shown in Fig. 7, in drained compression tests carried out here,
 408 suction evolves throughout the experiment and ends up with a lower value than the s_0 at the start

409 of the test. Therefore, the conditions of constant suction tests, typical of suction-controlled
410 oedometer tests, are not met here. Essentially, for the material tested here, it can be concluded that
411 the slope of compression curve decreases with increase of soil suction.

412 Fig. 14 presents variation of the C_{ae} with vertical net stress (σ_{vnet}) for unsaturated reconstituted
413 specimens. Similar to saturated reconstituted specimens (see Fig. 10), the C_{ae} , calculated for each
414 load increment, exhibits stress-dependency and increases with increase in σ_{vnet} . However, unlike
415 the saturated specimens, a peak value, after which the C_{ae} is decreased, is not apparent. In a rough
416 estimation, for specimens with s_0 of 362, 1405, 1907, and 21000 kPa, the maximum value of creep
417 index appears to occur at 710, 500, 500, and 400 kPa vertical total stress respectively. Furthermore,
418 increase of C_{ae} is small at low stress levels (< 200 kPa), and becomes larger at higher stress levels.
419 Moreover, it is clearly observed that increase in suction results in a decrease of the C_{ae} values.
420 With development of partial saturation state in the specimen during drying, the u_w becomes
421 negative at the back of the generated water menisci at the inter-particle contacts, applying tensile
422 pressure to the soil grains. The additional attractive forces exerted from the water menisci and
423 contractile skin, contribute to the reduction of particles' freedom for rearrangement under
424 sustained effective stress. The rate and magnitude of volumetric creep strains (ε_v^{cr}) are, therefore,
425 decreased with the increase in soil suction.



426

427

Fig. 14. Suction- and stress-dependency of C_{ae} for unsaturated reconstituted specimens

428 Fig. 15 presents the variation of C_{ae}/m'_c ratio with vertical net stress for unsaturated reconstituted

429 specimens. At low stress levels (< 200 kPa), the values of C_{ae}/m'_c decrease with increase in σ_{vnet} .

430 However, at higher stress levels, the values of C_{ae}/m'_c are scattered and do not follow a clear trend.

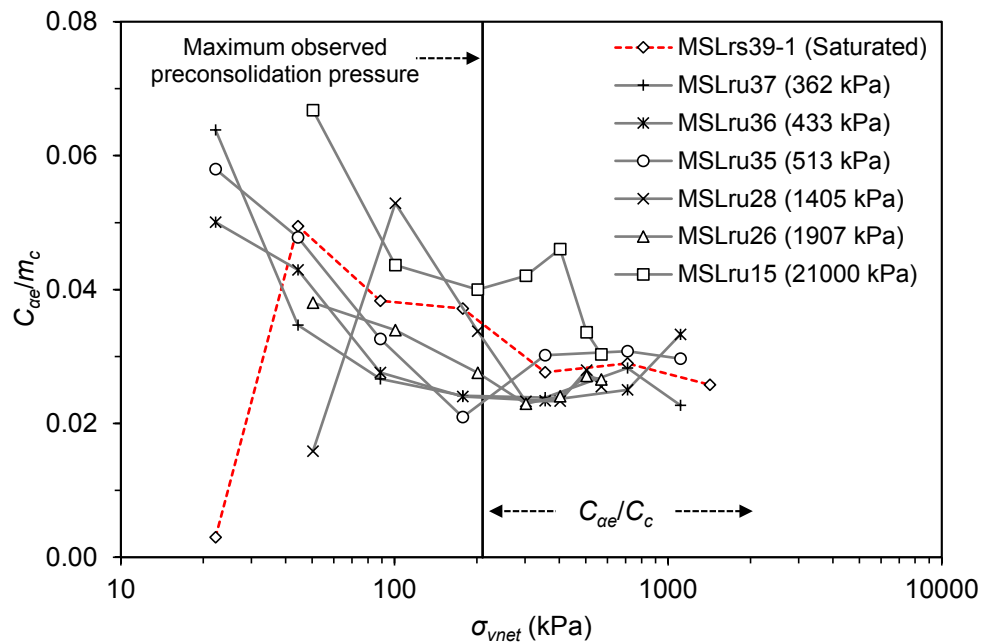
431 In a rough estimation, the values of $\alpha = C_{ae}/C_c$ could approximately be considered constant with

432 increase in stress level. Excluding the MSLru15 specimen, the values of α obtained for unsaturated

433 conditions appear to fall within a range of 0.023 – 0.030. Note that in saturated conditions, the

434 values of α decrease gradually to finally converge at a constant value of 0.024, whereas in

435 unsaturated conditions a clear trend and/or convergence is not observed.



436

437

Fig. 15. Suction- and stress-dependency of the α ratio for unsaturated reconstituted specimens

438 *Evaluation of α Ratio for Sheppey London Clay*

439 Table 4 summarises the stress ranges at which the maximum values of C_c , C_{ae} , and α occur for
 440 both intact and reconstituted specimens. The range and average values of α ratio obtained from
 441 different sets of experiments are also presented. The results indicate that for conventionally loaded
 442 intact specimens as well as reconstituted specimens with $w_0 = 0.39$, the maximum values of C_c
 443 and C_{ae} do not occur at the same stress level. However, for unconventionally loaded intact
 444 specimens as well as reconstituted specimens with $w_0 = 0.43$, C_c and C_{ae} reach the peak value at
 445 the same stress levels synchronously. The latter finding is in contradiction with the limited
 446 available observations reported in the literature for soft clays (see [Mataic et al. 2016](#)). The
 447 maximum values of α occur at stress levels in a range of $(1-2) \sigma'_p$, for both intact and reconstituted
 448 specimens. For unsaturated specimens, a peak value for C_c , C_{ae} , and α was not apparent. For
 449 saturated intact specimens, the range of α values varies significantly. For conventionally loaded
 450 intact specimens, an average α value of 0.03 ± 0.02 can be approximated. However, for
 451 unconventionally loaded intact specimens, a lower approximate average α value of 0.02 ± 0.01 is
 452 obtained. According to the classification criterion defined by [Mesri et al. \(1994\)](#), Sheppey London

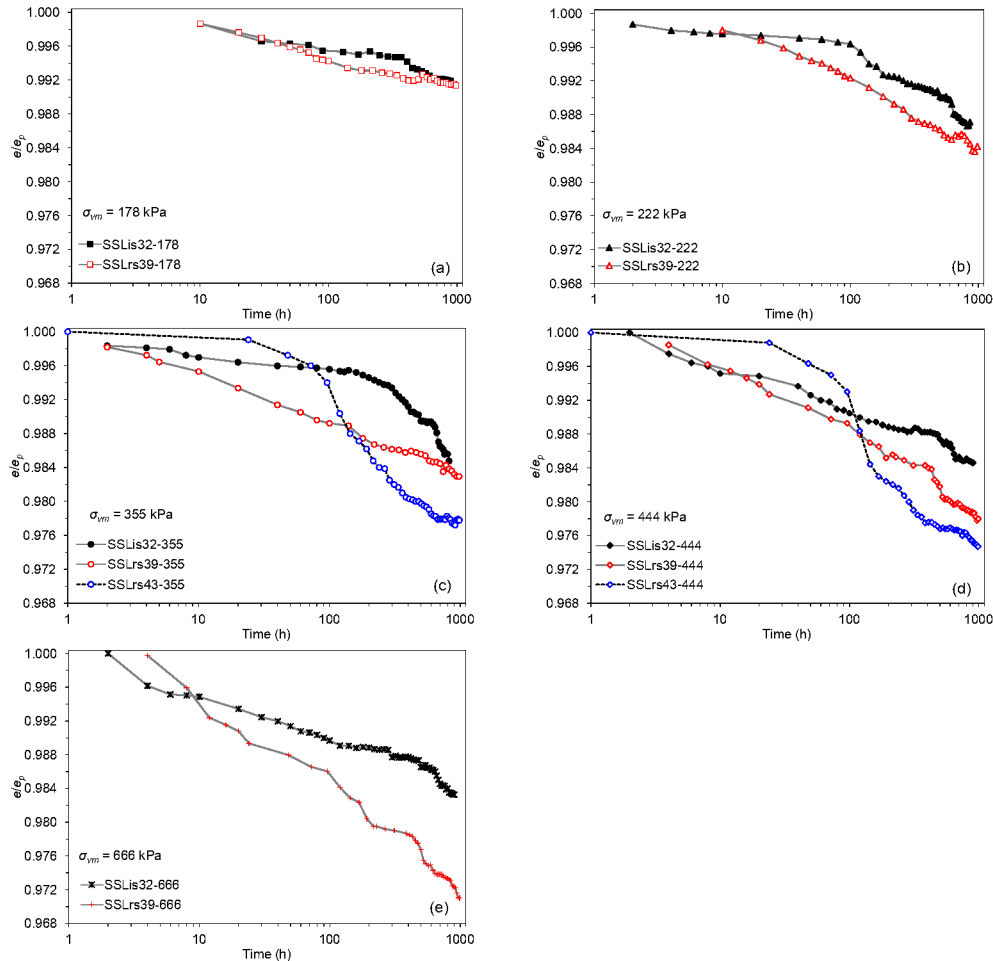
453 Clay lies in the zone of shale or mudstone whose α value ranges from 0.02 to 0.04. For saturated
454 and unsaturated reconstituted specimens, the ratio C_{ae}/C_c lies in a similar range of 0.023 – 0.037.
455 Accordingly, an average value of 0.03 ± 0.01 can be approximated for the α ratio of saturated and
456 unsaturated reconstituted specimens. The values of α for saturated LQU specimens fall in a range
457 of 0.023 – 0.048, with the lower band value being equal to that of reconstituted specimens, and
458 the upper band value, being similar to that of intact specimens.

459 ***Stress- and Suction-Dependent Response in SSL Tests***

460 Test results in this section are presented in plots of normalised void ratio e/e_p versus logarithm of
461 time, where e_p is the void ratio obtained 24 hours after the end of loading. The decision of
462 considering the results obtained after a period of 24 hours was made so as to ensure full dissipation
463 of u_{exc} , and also to allow for comparison between the results and define a criterion applicable to
464 all experiments. Similar approach was considered by [Cui et al. \(2009\)](#) for investigating time-
465 dependent behaviour of stiff Boom Clay.

466 Fig. 16 compares variation of the normalised void ratio e/e_p with logarithm of time for intact and
467 reconstituted specimens at different stress levels. For all specimens, higher volume changes were
468 observed with increase in σ_{vm} , indicating the stress-dependency of creep strains. The rate of change
469 in void ratio for all specimens was higher during the first 10 days of sustained loading, after which
470 it started to decrease. For intact and reconstituted specimens, the observed behaviour corresponds
471 to primary creep stage characterised as increasing creep strains at a decreasing strain-rate.
472 Furthermore, the creep rate and magnitude appears to be, in general, lower for intact specimens
473 than the reconstituted ones, this being, in part, due to the low w_0 of the intact specimens. Soil
474 structure, i.e. fabric anisotropy and inter-particle bonding, also plays a significant role in
475 controlling deformations. The process of destructuration during single-stage loading, and whether
476 the inter-particle bonds were fully or partly destroyed, is not, however, clearly identified.
477 Moreover, at the same stress level, the rate and magnitude of change in void ratio for reconstituted

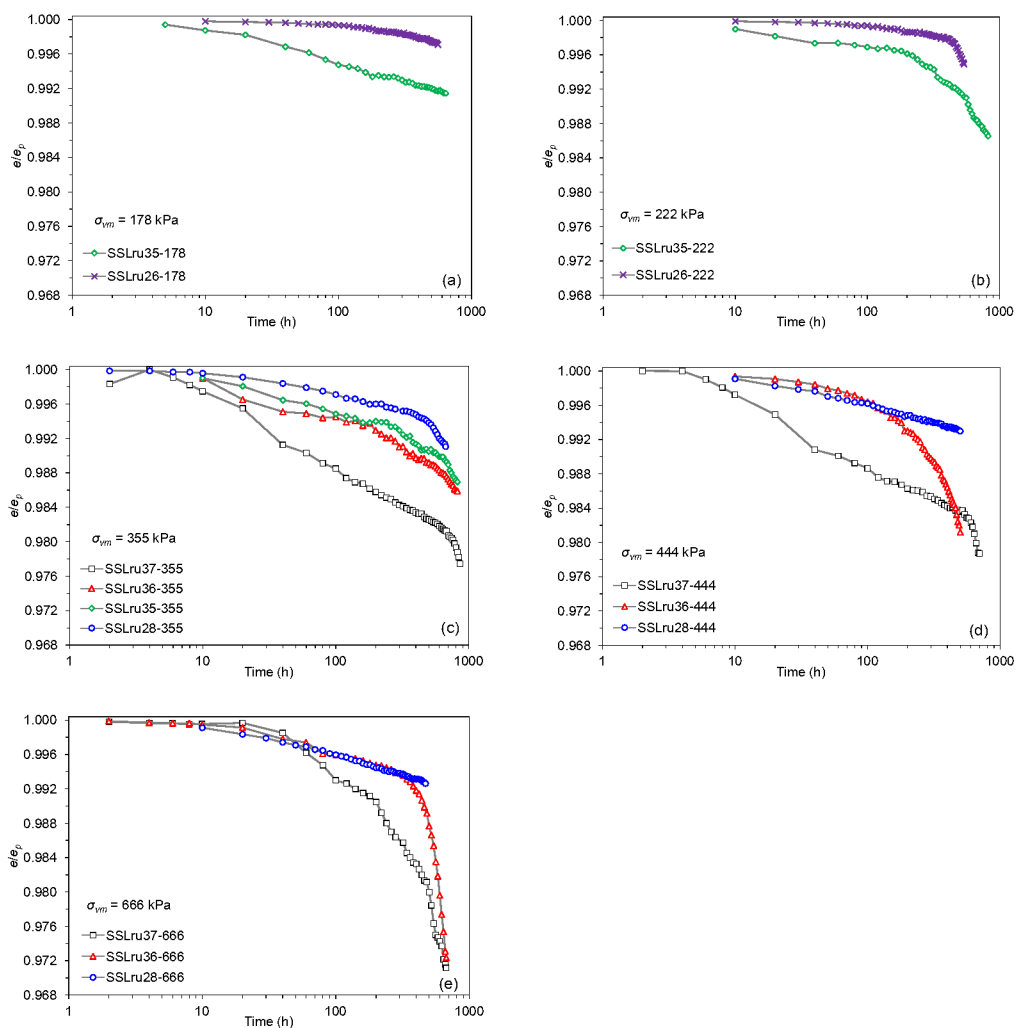
478 specimens with higher initial water contents ($w_0 = 0.43$) were found to be higher. In the absence
 479 of inter-particle bonds, the water content of the specimens appears to control the rate and
 480 magnitude of creep strains.



481 **Fig. 16.** SSL creep test results on intact and reconstituted specimens at stress levels of: (a) 178 kPa; (b)
 482 222 kPa; (c) 355 kPa; (d) 444 kPa; (e) 666 kPa

483 Graphs of Fig. 17 present the variation of normalised void ratio e/e_p with logarithm of time for
 484 specimens having different initial water contents (and therefore different suctions), and subjected
 485 to similar vertical stresses. It is clearly observed that at the same vertical stress level, decrease in
 486 w_0 (or increase in s_0) results in a decrease in the rate and magnitude of ε_v^{cr} . Unlike saturated soils,
 487 the water phase in partially-saturated soils is discontinuous. The generated water menisci between
 488 the soil particles hold the grains together and the soil particles are held together by the tensile

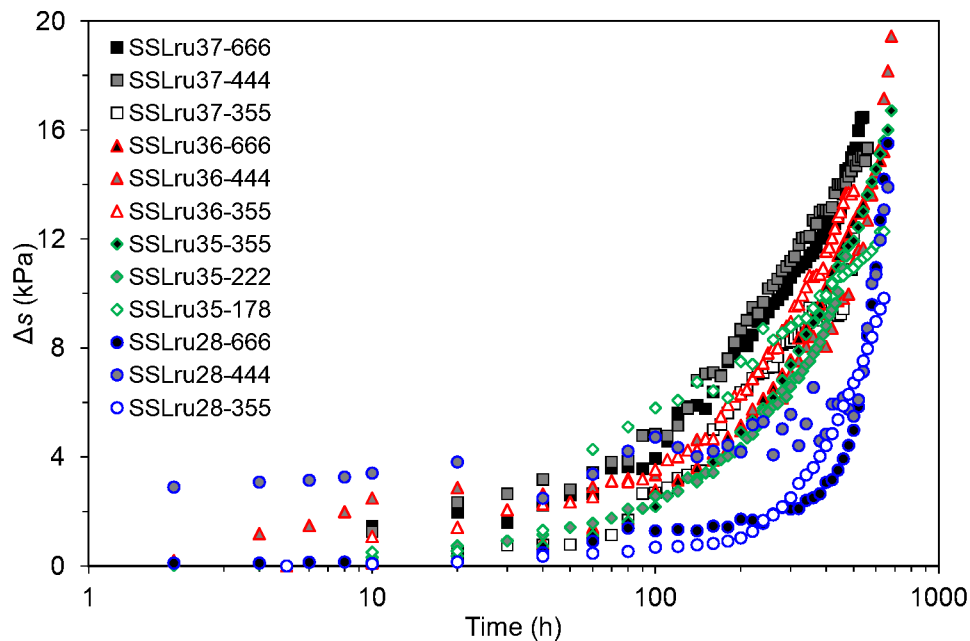
489 forces at the solid-water interface. During creep under constant effective stress, the under-tension
 490 water menisci resist against rearrangement and orientation of the clay particles.



491 **Fig. 17.** SSL creep test results on unsaturated reconstituted specimens at stress levels of: (a) 178 kPa; (b)
 492 222 kPa; (c) 355 kPa; (d) 444 kPa; (e) 666 kPa

493 Similar to saturated conditions (Fig. 16), creep behaviour in unsaturated conditions appears to be
 494 stress-dependent. However, effect of increase in σ_{vm} is more pronounced during the final stages of
 495 the unsaturated tests. For specimens SLLru28-444 and SLLru28-355 with $s_0 = 1405$ kPa, the
 496 volume change response appears to be fairly similar, indicating the predominant effect of soil
 497 suction in controlling creep deformations. Similar behaviour is also observed for SLLru26-222

498 and SSLru26-178 specimens with $s_0 = 1907$ kPa, further supporting this hypothesis. The
 499 predominant effect of suction is not, however, apparent for specimens with lower initial suctions.
 500 Similar to MSL tests, an instantaneous increase in u_w (decrease in suction) followed by a gradual
 501 pressure equalisation at each loading stage was observed. Moreover, for all loading stages, a
 502 suction state was preserved within the specimens, confirming that no water was expelled, and
 503 hence, the condition of constant water content was recognised throughout the loading stage. Fig.
 504 18 presents the results of monitoring suction evolutions during the creep stage of the tests. It is
 505 observed that suction is decreased with time for all of the test specimens. In fact, with increase in
 506 creep strains at constant water content, total volume is decreased resulting in an increase in the S_r ,
 507 which in turn, leads to a decrease in soil suction. This is, however, a possible mechanism, and the
 508 observed decrease in suction might be due to other factors influencing the HCTs measurements.
 509 However, if this is the case, keeping the soil suction constant during a constant suction creep test
 510 may not be ideal, as this may require a change (reduction) in S_r of the specimen, and hence,
 511 artificially development of creep strains.



512

513

Fig. 18. Monitoring suction changes during creep stage of SSL oedometer tests

514 **Conclusions**

515 Results of a set of MSL and SSL oedometer tests performed on Sheppey London Clay specimens
516 under different conditions of saturated intact, saturated reconstituted, and unsaturated
517 reconstituted were presented. The following conclusions can be drawn;

- 518 - The change in loading pattern, which was aimed at reducing the effects of sudden loading
519 and subsequent damages to the soil structure during MSL tests, does not have a notable
520 influence on the obtained compression curves and the C_r and C_c values for intact
521 specimens; however, it leads to lower C_{ae}/C_c values than the conventionally loaded
522 specimens.
- 523 - Unlike soft clays that exhibit a sudden increase of C_c in the post yield region due to
524 structural collapse, the process of destructuration in stiff LC appears to be continuous and
525 follows an almost linear trend.
- 526 - Unlike natural soft clays which typically exhibit higher creep than their corresponding
527 reconstituted specimens, stiff LC exhibits significantly less creep in comparison with the
528 corresponding reconstituted specimens. This, on the one hand, can be attributed to the more
529 compact nature of stiff clays (low e_0), and on the other hand, to the low w_0 of the intact
530 specimens.
- 531 - Generally, for Sheppey LC, increase in suction results in a decrease in the slope of
532 compression curve (m'_c) and the C_{ae} values, and an increase in σ_p .
- 533 - According to the classification criterion defined by [Mesri et al. \(1994\)](#), Sheppey LC is
534 categorised as shale or mudstone whose α value ranges from 0.02 to 0.04. The $\alpha = C_{ae}/C_c$
535 ratio for Sheppey LC is stress- and suction-dependent, and therefore cannot be considered
536 as a constant value. However, as a rough estimation, an average value of 0.03 ± 0.01 can
537 be approximated for the α ratio of saturated and unsaturated reconstituted specimens.

- 538 - During SSL tests, at the same vertical stress level, decrease in w_0 (or increase in s_0) results
539 in a decrease in the rate and magnitude of ε_v^{cr} . Moreover, at the same s_0 , increase in applied
540 vertical stress leads to an increase in the ε_v^{cr} .
- 541 - The volume change of specimens with high s_0 during SSL tests appears to be
542 predominantly controlled by the state of suction stress rather than the applied vertical
543 stress.
- 544 - During long-term creep tests at constant water content, a decrease in soil suction monitored
545 by HCTs can be attributed to an increase in S_r of the specimen with decrease in total volume
546 during creep. If this holds true, long-term creep tests where suction is artificially kept
547 constant may not be ideal and the observed creep strains may not be solely attributed to
548 the applied total vertical stress.
- 549 - Further investigations and more test results over a wider range of soil suction and applied
550 vertical stress levels are required to validate the observed time-dependent response for the
551 tested soil.
- 552

553 **References**

- 554 Alonso, E.E., Gens, A. and Josa, A. 1990. A constitutive model for partially saturated soils.
555 *Géotechnique*, **40**(3): 405–430. doi: 10.1680/geot.1990.40.3.405.
- 556 Bagheri, M., Rezaia, M. and Mousavi Nezhad, M. 2015. An experimental study of the initial
557 volumetric strain rate effect on the creep behaviour of reconstituted clays. IOP Conference
558 Series: Earth and Environmental Science, **26**(1): 012034.
- 559 Bagheri, M., Rezaia, M. and Mousavi Nezhad, M. 2018. Cavitation in high-capacity
560 tensiometers: effect of water reservoir surface roughness. *Geotechnical Research*, **5**(2):
561 81–95. doi: 10.1680/jgere.17.00016.
- 562 Bagheri, M., Mousavi Nezhad, M., and Rezaia, M. 2019a. A CRS oedometer cell for unsaturated
563 and non-isothermal tests. *Geotechnical Testing Journal*, **43**(1), in press. doi:
564 10.1520/GTJ20180204.
- 565 Bagheri, M., Rezaia, M., and Mousavi Nezhad, M. 2019b. Rate-dependency and stress relaxation
566 of unsaturated clays, *International Journal of Geomechanics*, In Press.
- 567 Cui, Y.-J., Le, T.T., Tang, A.M., Delage, P. and Li, X.L. 2009. Investigating the time-dependent
568 behaviour of Boom clay under thermomechanical loading. *Géotechnique*, **59**(4): 319–329.
569 doi: 10.1680/geot.2009.59.4.319.
- 570 De Gennaro, V., Delage, P., Cui, Y.J., Schroeder, C. and Collin, F. 2003. Time-dependent
571 behavior of oil reservoir chalk: a multiphase approach. *Soils and Foundations*, **43**(4): 131–
572 147. doi: 10.3208/sandf.43.4_131.
- 573 De Gennaro, V., Sorgi, C. and Delage, P. 2005. Air-water interaction and time dependent
574 compressibility of a subterranean quarry chalk. Paper presented in Symposium Post
575 Mining, Nancy, France, pp. 1–12.
- 576 Delage, P., Le, T.T., Tang, A.M., Cui, Y.J. and Li, X.L. 2007. Suction effects in deep Boom Clay
577 block samples. *Géotechnique*, **57**(2): 239–244. doi: 10.1680/geot.2007.57.2.239.

- 578 Fredlund, D.G. and Xing, A. 1994. Equations for the soil-water characteristic curve. Canadian
579 Geotechnical Journal, **31**(3): 521–532. doi: 10.1139/t94-061.
- 580 Fredlund, D.G. 2006. Unsaturated soil mechanics in engineering practice, Journal of Geotechnical
581 and Geoenvironmental Engineering, **132**(3): 286–321. doi: 10.1061/(ASCE)1090-
582 0241(2006)132:3(286)
- 583 Gasparre, A. 2005. Advanced laboratory characterisation of London Clay. Ph.D. Thesis, University
584 of London.
- 585 Karstunen, M. and Yin, Z.-Y. 2010. Modelling time-dependent behaviour of Murro test
586 embankment. Géotechnique, **60**(10): 735–749. doi: 10.1680/geot.8.P.027.
- 587 Lai, X., Wang, S., Qin, H. and Liu, X. 2010. Unsaturated creep tests and empirical models for
588 sliding zone soils of Qianjiangping landslide in the Three Gorges. Journal of Rock
589 Mechanics and Geotechnical Engineering, **2**(2): 149–154. doi:
590 10.3724/SP.J.1235.2010.00149.
- 591 Li, J.Z., Peng, F.L. and Xu, L.S. 2009. One-dimensional viscous behavior of clay and its
592 constitutive modeling. International Journal of Geomechanics, **9**(2): 43–51. doi:
593 10.1061/(ASCE)1532-3641(2009)9:2(43).
- 594 Li, J.Z., Peng, F.L., Xu, L.S. and Tatsuoka, F. 2006. Viscous properties of clay with different
595 water content. Soil and rock behavior and modeling (GSP 150), ASCE, **194**: 55–61. doi:
596 10.1061/40862(194)6.
- 597 Li, J.-Z., Tatsuoka, F., Nishi, T. and Komoto, N. 2003. Viscous stress-strain behaviour of clay
598 under unloaded conditions. *In* Proceedings of the 3rd International Symposium on
599 Deformation Characteristics of Geomaterials: IS Lyon 03, Lyon, France, pp. 617–625.
- 600 Mataic, I., Wang, D. and Korkiala-Tanttu, L. 2016. Effect of destructuration on the compressibility
601 of Pernio clay in incremental loading oedometer tests. International Journal of
602 Geomechanics, **16**(1): 040150161. doi: 10.1061/(ASCE)GM.1943-5622.0000486.

- 603 Mesri, G. and Castro, A. 1987. C_d/C_c concept and K_0 during secondary compression. Journal of
604 Geotechnical Engineering, **113**(3): 230–247. doi: 10.1061/(ASCE)0733-
605 9410(1987)113:3(230).
- 606 Mesri, G. and Godlewski, P. M. 1977. Time and stress-compressibility interrelationship. Journal
607 of Geotechnical Engineering Division, American Society of Civil Engineers, **103**(5):
608 417–430.
- 609 Mesri, G., Kwan, L.D.O., and Feng, W.T. 1994. Settlement of embankment on soft clays. *In*
610 Proceedings of the Conference on Vertical and Horizontal Deformations of Foundations
611 and Embankments: Part 2 (of 2), College Station, TX, USA, American Society of Civil
612 Engineers, GSP 1(40), pp. 8–56.
- 613 Mesri, G. 2009. Discussion of ‘Effects of friction and thickness on long-term consolidation
614 behavior of Osaka Bay clays’ by Watabe, Udaka, Kobayashi, Tabata & Emura 2008. Soils
615 and Foundation., **49**(5): 823–824.
- 616 Monroy, R., Zdravkovic, L. and Ridley, A.M. 2008. Volumetric behaviour of compacted London
617 Clay during wetting and loading. *In* Proceedings of the 1st European Conference on
618 Unsaturated Soils, E-UNSAT 2008, Durham, UK, pp. 315–320.
- 619 Nazer, N.S.M., and Tarantino, A. 2016. Creep response in shear of clayey geo-materials under
620 saturated and unsaturated conditions. *In* Proceedings of the 3rd European Conference on
621 Unsaturated Soils, E-UNSAT 2016, Paris, France, pp. 1–5.
- 622 Oldecop, L.A., and Alonso, E.E. 2007. Theoretical investigation of the time-dependnet behaviour
623 of rockfill. Géotechnique, **57**(3): 289–301. doi: 10.1680/geot.2007.57.3.289.
- 624 Pereira, J.M. and De Gennaro, V. 2010. On the time-dependent behaviour of unsaturated
625 geomaterials. *In* Proceedings of the 5th International Conference on Unsaturated Soils,
626 Barcelona, Spain, pp. 921–925.

- 627 Priol, G., De Gennaro, V., Delage, P. and Servant, T. 2007. Experimental investigation on the time
628 dependent behavior of a multiphase chalk. *In* Experimental unsaturated soil mechanics.
629 Edited by T. Schanz, Springer Proceedings Physics 112, pp. 161–167.
- 630 Rezania, M., Bagheri, M., Mousavi Nezhad, M. and Sivasithamparam, N. 2017. Creep analysis of
631 an earth embankment on soft soil deposit with and without PVD improvement. *Geotextiles*
632 *and Geomembranes* **45**(5): 537–547. doi: 10.1016/j.geotexmem.2017.07.004.
- 633 Sivakumar, V. 1993. A critical state framework for unsaturated soil. Ph.D. Thesis, University of
634 Sheffield, UK.
- 635 Sorensen, K.K. 2006. Influence of viscosity and ageing on the behaviour of clays. Ph.D. Thesis,
636 University College London.
- 637 Wheeler, S. J. and Sivakumar, V. 1995. An elasto-plastic critical state framework for unsaturated
638 soil. *Géotechnique*, **45**(1): 35–53. doi: 10.1680/geot.1995.45.1.35.
- 639 Yin, J.-H. and Feng, W.-Q. 2017. A new simplified method and its verification for calculation of
640 consolidation settlement of a clayey soil with creep. *Canadian Geotechnical Journal*, **54**(3):
641 333–347. doi: 10.1139/cgj-2015-0290.
- 642 Yin, Z.-Y., Karstunen, M., Chang, C.S., Koskinen, M. and Lojander, M. 2011. Modeling time-
643 dependent behavior of soft sensitive clay. *Journal of Geotechnical and Geoenvironmental*
644 *Engineering*, **137**(11): 1103–1113. doi: 10.1061/(ASCE)GT.1943-5606.0000527.
- 645 Zhou, A.N., Sheng, D., Sloan, S.W. and Gens, A. 2012. Interpretation of unsaturated soil
646 behaviour in the stress–saturation space, I: Volume change and water retention behaviour.
647 *Computers and Geotechnics*, **43**: 178–187. doi: 10.1016/j.compgeo.2012.04.010.
- 648
- 649

650 **List of Symbols**

- C_c = compression index in $e - \log \sigma'_v$ space
 C_r = reloading index in $e - \log \sigma'_v$ space
 C_s = swelling index in $e - \log \sigma'_v$ space
 C_{ae} = creep index with respect to e
 e = void ratio
 e_0 = initial void ratio
 e_i = instantaneous change in void ratio
 e_p = void ratio 24 hours after the end of loading in SSL tests
 G_s = specific gravity
 I_p = plasticity index
 k_v = coefficient of vertical permeability
 m'_c = slope of compression curve in $e - \log \sigma_v$ space for unsaturated conditions
 m_c = slope of compression curve in $e - \log \sigma'_v$ space for saturated conditions
 S_r = degree of saturation
 s = soil suction
 s_0 = initial suction
 t = time
 u_a = pore-air pressure
 u_{exc} = excess pore-water pressure
 u_w = pore-water pressure
 w = gravimetric water content
 w_0 = initial gravimetric water content
 w_L = liquid limit
 w_P = plastic limit
 α = represents the ratio C_{ae}/C_c
 β = represents the ratio e_i/e_p
 ε_v^{cr} = volumetric creep strain
 σ_p = yield vertical net stress in unsaturated states
 σ'_p = yield vertical net stress in saturated states
 σ_v = applied vertical total stress
 σ'_v = vertical effective stress
 σ_{vm} = maximum applied vertical stress
 σ_{vnet} = net normal stress

652 **List of Tables**

653

654 **Table 1.** Physical properties of Sheppey London Clay samples

Clay (%)	Silt (%)	Sand (%)	<i>in-situ</i> w (%)	w_P (%)	w_L (%)	G_s	k_v (m/s) at 20° C
64	34	2	29 – 35	19 – 24	70 – 78	2.67	2.5×10^{-10}

655

Table 2. Details of MSL tests

Test ID	Loading/unloading stresses (kPa)	w_0 (%)	s_0 (kPa)	σ_{vm} (kPa)	Test duration (days)	Test condition
MSLis32-1	22-44-89-178-355-710-1421-710-355-178-89	32		1421	11	Saturated
MSLis32-2	22-44-89-178-355-710-1421-710-355-178-89	32		1421	11	
MSLis32-3	22-44-89-178-355-710-1421-710-355-178-89	32		1421	11	
MSLis32-4	11-22-44-89-178-222-333-444-666-888-1110-1332-1110-888-666-444-333-222-178	32		1332	19	
MSLis32-5	11-22-44-89-178-222-333-444-666-888-1110-1332-1110-888-666-444-333-222-178	32		1332	19	
MSLis32-6	11-22-44-89-178-222-333-444-666-888-1110-1332-1110-888-666-444-333-222-178	32		1332	19	
MSLis32-7*	22-44-89-133-178-222-333-444-666-888-1110-888-666-444-333-222-178-133	32		1110	18	
MSLis32-8*	22-44-89-133-178-222-333-444-666-888-1110-888-666-444-333-222-178-133	32		1110	18	
MSLis32-9*	22-44-89-133-178-222-333-444-666-888-1110-888-666-444-333-222-178-133	32		1110	18	
MSLrs39-1	11-22-44-89-178-355-710-1421-710-355-178-44	39		1421	12	
MSLrs39-2	11-22-44-89-178-355-710-1421-710-355-178-44	39		1421	12	
MSLrs39-3	11-22-44-89-178-355-710-1421-710-355-178-44	39		1421	12	
MSLrs43-1	11-22-44-89-178-355-710-1421-710-355-178-44	43		1421	12	
MSLrs43-2	11-22-44-89-178-355-710-1421-710-355-178-44	43		1421	12	
MSLrs43-3	11-22-44-89-178-355-710-1421-710-355-178-44	43		1421	12	
MSLru37	22-44-89-178-355-710-1110-710-355-178-89-44-22-11	37	326	1111	14	Unsaturated
MSLru36	22-44-89-178-355-710-1110-710-355-178-89-44-22-11	36	433	1111	14	
MSLru35	22-44-89-178-355-710-1110-710-355-178-89-44-22-11	35	513	1111	14	
MSLru28	25-50-100-200-300-400-500-580-500-400-300-200-100-50-25	28	1405	605	15	
MSLru26	25-50-100-200-300-400-500-580-500-400-300-200-100-50-25	26	1907	605	15	
MSLru15	25-50-100-200-300-400-500-580-500-400-300-200-100-50-25	15	~21000	605	15	

r: reconstituted, i: intact, s: saturated, u: unsaturated, *: low-quality undisturbed
 The number before dash indicates initial water content and the number after dash indicates the test number.

658

Table 3. Details of SSL creep oedometer tests

Test ID	w_0 (%)	s_0 (kPa)	σ_{vm} (kPa)	Test duration (days)	Test conditions
SSLis32-178	32		178	37	Saturated
SSLis32-222	32		222	36	
SSLis32-355	32		355	36	
SSLis32-444	32		444	38	
SSLis32-666	32		666	38	
SSLrs39-178	39		178	60	
SSLrs39-222	39		222	68	
SSLrs39-355	39		355	68	
SSLrs39-444	39		444	46	
SSLrs39-666	39		666	46	
SSLrs43-355	43		355	94	Unsaturated
SSLrs43-444	43		444	94	
SSLru37-666	37	326	666	28	
SSLru37-444	37	326	444	29	
SSLru37-355	37	326	355	36	
SSLru36-666	36	433	666	28	
SSLru36-444	36	433	444	21	
SSLru36-355	36	433	355	34	
SSLru35-355	35	513	355	34	
SSLru35-222	35	513	222	34	
SSLru35-178	35	513	178	27	
SSLru28-666	28	1405	666	20	
SSLru28-444	28	1405	444	21	
SSLru28-355	28	1405	355	28	
SSLru26-222	26	1907	222	23	
SSLru26-178	26	1907	178	23	

The number after dash shows the σ_{vm} .

659

660

661

662

663

664

665

666

667

668

669

670

Table 4. Stress ranges for maximum C_c , C_{ae} , and α parameters

Test ID	σ'_v / σ'_p or σ_v / σ_p			Range of α values	Average α
	$(C_c)_{\max}$	$(C_{ae})_{\max}$	$(\alpha)_{\max}$		
MSLis32-1					
MSLis32-2	8 – 10	6 – 7	1 – 2	0.015 – 0.046	0.031 ± 0.016
MSLis32-3					
MSLis32-4					
MSLis32-5	8 – 10	8 – 11	1 – 2	0.017 – 0.031	0.024 ± 0.007
MSLis32-6					
MSLis32-7*					
MSLis32-8*	6 – 8	4 – 5	4 – 5	0.023 – 0.048	0.036 ± 0.013
MSLis32-9*					
MSLrs39-1					
MSLrs39-2	3 – 4	6 – 7	1 – 2	0.022 – 0.037	0.03 ± 0.008
MSLrs39-3					
MSLrs43-1					
MSLrs43-2	3 – 4	3 – 4	1 – 2	0.024 – 0.036	0.03 ± 0.006
MSLrs43-3					
MSLru37					
MSLru28	3 – 4	2 – 5	NA	0.023 – 0.037	0.03 ± 0.007
MSLru26					
MSLru36					
MSLru35	NA	NA	NA	0.023 – 0.045	0.034 ± 0.011
MSLru15					

671

672

673 **Figure Captions**

674 **Fig. 1** SWRC determined for main drying path

675 **Fig. 2.** Schematic diagram of the unsaturated oedometer cell

676 **Fig. 3.** Comparison of the compression curves for intact Sheppey LC and natural LC from Unit C
677 of Heathrow T5 site

678 **Fig. 4.** Comparison of the compression curves for reconstituted Sheppey LC and natural LC from
679 Unit C of Heathrow T5 site

680 **Fig. 5.** Comparison of the compression curves for saturated intact, reconstituted, and LQU
681 specimens

682 **Fig. 6.** Compression curves for unsaturated reconstituted specimens

683 **Fig. 7.** Monitoring suction changes during step loading oedometer tests

684 **Fig. 8.** Evolution of Skempton B value with vertical net stress

685 **Fig. 9.** Stress-dependency of the slope of compression curve for saturated intact, reconstituted,
686 and LQU specimens

687 **Fig. 10.** Stress-dependency of C_{ae} for intact, reconstituted, and LQU specimens

688 **Fig. 11.** Stress-dependency of C_{ae}/C_c for intact, reconstituted, and LQU specimens

689 **Fig. 12.** Suction- and stress-dependency of the slope of compression curve for unsaturated
690 reconstituted specimens

691 **Fig. 13.** Variation of C_c and C_s with suction for unsaturated reconstituted specimens

692 **Fig. 14.** Suction- and stress-dependency of C_{ae} for unsaturated reconstituted specimens

693 **Fig. 15.** Suction- and stress-dependency of the α ratio for unsaturated reconstituted specimens

694 **Fig. 16.** SSL creep test results on intact and reconstituted specimens at stress levels of: (a) 178
695 kPa; (b) 222 kPa; (c) 355 kPa; (d) 444 kPa; (e) 666 kPa

696 **Fig. 17.** SSL creep test results on unsaturated reconstituted specimens at stress levels of: (a) 178
697 kPa; (b) 222 kPa; (c) 355 kPa; (d) 444 kPa; (e) 666 kPa

698 **Fig. 18.** Monitoring suction changes during creep stage of SSL oedometer tests

17 Abstract

18 In this paper the one-dimensional (1D) time-dependent behaviour of natural and reconstituted
19 London Clay samples under saturated and unsaturated conditions is studied. For this purpose, a
20 set of 1D consolidation tests including multi-staged loading (MSL) oedometer tests and single-
21 staged loading (SSL) long-term oedometer creep tests were carried out on saturated and
22 unsaturated specimens. Conventional oedometer cells were used for tests on saturated specimens,
23 whereas a newly designed unsaturated oedometer cell, equipped with two high-capacity
24 tensiometers (HCTs) for suction measurements, was used for unsaturated tests. The tests results
25 revealed stress- and suction-dependency of primary and secondary consolidation responses of the
26 soil samples. Furthermore, counter to formerly acknowledged suggestions of independency of the
27 slope of normal consolidation line to suction changes, it was observed that an increase in suction
28 results in a decrease of the slope of compression curve (C_c) and the creep index (C_{ae}) values, and
29 an increase in yield vertical net stress (σ_p). Moreover, the C_{ae}/C_c ratio for London Clay was found
30 to be stress- and suction-dependent, unlike the previously suggested hypotheses.

31 **Keywords:** Stiff clay, Creep, Oedometer, Suction, Unsaturated soils

32

33 **Introduction**

34 Experimental investigations have proven dependency of the mechanical behaviour of clays on
35 time effects (Li et al. 2003; Mesri 2009; Karstunen and Yin 2010; Bagheri et al. 2015; Yin and
36 Feng 2017; Rezania et al. 2017; Bagheri et al. 2019b). These effects are commonly observed as
37 post-construction deformations of gestructures such as roads, railways, and dams. The time-
38 dependency of mechanical response is usually observed through irreversible creep deformations
39 which are typically coupled with external sources of deformations driven by, for example, repeated
40 loadings, rainfalls, flooding, and earthquakes (Oldecop and Alonso 2007). The main focus of the
41 reported works in the literature has been laid on characterisation of creep deformations in saturated
42 soft clays. This is while the shallow depth soil layers, typically studied for practical engineering
43 purposes, are usually found in partially-saturated states. Little is currently known about the
44 compression and creep response of unsaturated clays, in particular stiff clays such as London Clay
45 (LC). The reported works on creep response in unsaturated conditions are limited to observations
46 of time-dependent volume change behaviour of reservoir chalks (De Gennaro et al. 2003; De
47 Gennaro et al. 2005; Priol et al. 2007; Pereira and De Gennaro 2010), rockfills (Oldecop and
48 Alonso 2007), and reconstituted clays (Lai et al. 2010; Nazer and Tarantino 2016). Priol et al.
49 (2007) performed a set of multi-staged loading creep oedometer tests on oil-saturated, water-
50 saturated, partially-saturated, and dry Lixhe chalk (an outcrop chalk from Belgium) and reported
51 that at high pressures the creep index (C_{ae}) values increased with increase in vertical stress and
52 decreased with increase in suction (s). Similar results were reported by De Gennaro et al. (2005)
53 who evaluated the suction- and stress-dependency of creep index in MSL compression tests on
54 Estreux chalk under dry, water-saturated, and unsaturated ($s = 1.5$ MPa) conditions using a
55 suction-controlled osmotic oedometer cell. The results of unsaturated triaxial drained creep tests
56 performed on sliding zone soils of the Qianjiangping landslide (Lai et al. 2010) demonstrated that
57 an increase in matric suction results in a decrease in creep strain rate and magnitude under constant
58 net confining pressure and deviatoric stress. However, despite practical interests, generalisation of

59 these findings to various soil types, stress states, and suction ranges and coupling partial saturation
60 states and time effects is still an open topic.

61 This paper presents the results of multi-staged loading (MSL) and single-stage loading (SSL)
62 oedometer creep tests performed on saturated and unsaturated LC specimens. Saturated tests were
63 performed on undisturbed and reconstituted specimens, whereas the unsaturated creep tests were
64 performed only on reconstituted specimens. The results of MSL tests are discussed with emphasis
65 on the effects of soil structure, suction, and vertical stress level on the compression response,
66 consolidation indices, and C_{ae}/C_c ratio. The effects of suction and vertical stress level on
67 volumetric creep strains are further discussed based on the results of SSL oedometer tests.

68 **Material and Apparatus**

69 The test material is London Clay extracted from the New Hook Farm in Isle of Sheppey in the
70 UK. Undisturbed block samples of un-weathered LC were taken at 4 m depth below non-quarried
71 ground level. The index parameters and physical properties of the natural samples are summarised
72 in Table 1. Laboratory determination of index parameters confirmed the upper bound values of
73 24% and 78% for respectively plastic limit (w_p) and liquid limit (w_L) indices. Based on the USCS
74 classification, the samples are classified as clay of high plasticity (CH).

75 The particle size distribution (PSD) curve of natural LC presents 98% particles passing through
76 the 0.063 mm sieve. The high content of fine grain inclusions results in an air-entry value (AEV)
77 of several megapascals (e.g. [Monroy et al. 2008](#)). In order to decrease the AEV, the PSD was
78 modified by including larger sized aggregates, resulting from crushing the oven-dried samples,
79 and passing through 1.18 mm sieve. The soil water retention curve (SWRC) and AEV of the
80 sample with modified PSD were measured using axis-translation and high-capacity tensiometer
81 (HCT) techniques following the procedure outlined in [Bagheri et al. \(2019a\)](#). As shown in Fig. 1,
82 the modified sample exhibited an AEV of around 260 kPa which allows for testing specimens over

83 a wider range of suctions lying on the transition (de-saturation) phase of the SWRC. It must be
84 noted here that, although it is desired to obtain the AEV from a plot of degree of saturation versus
85 suction, reliable values for the AEV can be also derived from the plot of water content versus
86 suction ([Fredlund 2006](#)).

87 Undisturbed oedometer specimens were directly cored from the block samples using a 75 mm
88 diameter and 20 mm high oedometer ring. The inner wall of the ring was slightly lubricated with
89 grease before preparing the specimen, in order to minimise the side friction effects on the stress–
90 strain response. Reconstituted soil samples were prepared by mixing the soil powder, containing
91 the large-sized aggregates, with distilled water at $1.5w_L$. The slurry was then consolidated in a 100
92 mm diameter Perspex consolidometer under a vertical stress of 80 kPa for a duration of 5 days.
93 The samples were then quickly unloaded to minimise swelling and water absorption. Reconstituted
94 saturated specimens were cored from the obtained cylindrical soil cakes. Unsaturated specimens
95 were cored from smaller subsamples air-dried at room temperature to pre-specified water contents
96 and stored in air-tight containers for a duration of one week to attain moisture equilibrium.
97 Selection of the initial water contents (w_0) of the specimens was based on the information obtained
98 from the developed SWRC for reconstituted samples and to examine compressibility of specimens
99 with a wide range of suctions on the transition effect zone (partially saturated zone) of the main
100 drying curve.

101 Saturated tests were carried out in conventional oedometer cells, whereas unsaturated tests were
102 carried out in suction-monitored oedometer cells equipped with two high-capacity tensiometers
103 (HCTs) for monitoring suction evolutions ([Bagheri et al. 2018](#)). The special design of the
104 oedometer loading cap allows for replacement of a cavitating HCT without any disturbance to the
105 specimen and interruption in measurement of deformations. A schematic view of the unsaturated
106 oedometer cell is provided in Fig. 2.

107

108 **Experimental Program**

109 MSL oedometer tests with 24 hour loading periods were performed on intact, reconstituted, and
110 low-quality undisturbed (LQU) specimens. Considering the fissured nature of the LC, significant
111 attention was given during the preparation of intact specimens. Where the specimen preparation
112 process involved minor visible damage to the soil structure, the prepared specimen was marked as
113 LQU. Prior to the start of the tests, the w_0 and the specimen dimensions were measured for
114 saturated MSL tests. The specimen was then set in the conventional oedometer cell and vertical
115 load was applied step-wise to the submerged specimen during each 24 hours loading step.
116 Typically, for conventional oedometer tests, vertical load is doubled at each stage of loading. This
117 can, however, cause significant unfavourable disturbance to the structural properties of the test
118 specimen especially at high stress levels. In order to reduce such effects, in addition to the doubling
119 vertical stress method, other loading patterns, as shown in Table 2, were also considered. By the
120 end of loading to the desired stress levels, the specimens were unloaded step-wise in order to
121 evaluate the swelling response. Each unloading stage was kept for 24 hours to ensure complete
122 swelling and that most of the generated suction was released. The compression curves were finally
123 obtained based on the final settlement values. For unsaturated MSL tests, prior to each experiment,
124 the HCTs were saturated and preconditioned following the procedure explained by [Bagheri et al.](#)
125 [\(2018\)](#). In order to ensure ultimate contact between the specimen and the HCTs, the ceramic disks
126 of the tensiometers were covered with soil paste, and a small vertical stress was also applied to the
127 specimen. The average suction recorded by the two HCTs, used to monitor suction changes, at the
128 start of loading was considered as the initial suction (s_0) of the specimen. In all experiments, the
129 pressure difference recorded by the two HCTs did not exceed 5 kPa. The HCTs were also
130 periodically calibrated in order to account for any possible changes in their performance. For
131 specimens with s_0 values beyond the capacity of the HCTs, the corresponding s_0 values were
132 estimated from the curve fitting of the experimental SWRC using [Fredlung and Xing \(1994\)](#)
133 equation. Table 2 presents the details of MSL tests.

134 SSL tests were carried out only on reconstituted specimens in order to avoid the complexities
135 associated with coupled effects of suction and soil structure. Unlike conventional incremental
136 loading tests, the test pressure was applied directly in a single loading stage in order to remove the
137 possible effects of loading and creep history on the measured creep strains. Moreover, in order to
138 avoid the problems associated with sudden loading, the applied pressure was ramped up to the
139 desired vertical stress level at a constant rate of 8-10 kPa per hour. The applied pressure was
140 sustained for a period of 19 to 94 days. The values of the maximum applied vertical stresses (σ_{vm})
141 were chosen so that they were higher than the preconsolidation pressure of the samples so that it
142 was possible to investigate the creep response in the normal consolidation state. Unsaturated tests
143 were conducted on specimens having initial suction states on the main drying curve of the SWRC
144 in order to eliminate the complexity associated with volumetric deformation due to wetting
145 (wetting-induced deformations or collapse in wetting), and therefore observe the effect of suction
146 on mechanically induced creep deformations. Details of the carried out experiments are
147 summarised in Table 3.

148 **Results**

149 The compression index (C_c), swelling index (C_s), and reloading index (C_r) values were calculated
150 as the slope of respectively the normal compression line (NCL), the swelling (unloading) line, and
151 the reloading line of the compression curve plotted in $e - \log \sigma'_v$ space, where e is void ratio and
152 σ'_v is vertical effective stress. As suggested by [Mataic et al. \(2016\)](#), the creep index (C_{ae}) was
153 defined as the slope of the plot of void ratio versus logarithm of time (t) from the time period of
154 6–24 hours for each load increment. The decrease in void ratio during this time scale represents
155 the creep phase as the end of primary consolidation (EOP) was found to be within the first 5–6
156 hours of each loading increment. The experimental results of unsaturated oedometer tests can be
157 evaluated based on the generalised vertical effective stress relationship;

$$(1) \quad \sigma'_v = \sigma_{vnet} + S_r s$$

158 where S_r is the degree of saturation, s is soil suction, and $\sigma_{vnet} = \sigma_v - u_a$ is the net normal stress
 159 defined as the difference of vertical total stress (σ_v) and pore-air pressure (u_a). Estimation of S_r
 160 requires the information of the water content of the specimen during the test. However, as the
 161 suction-monitored oedometer cell does not allow for measurement of the specimens' water
 162 content, the experimental results of unsaturated oedometer tests were evaluated based on the σ_{vnet} ,
 163 and since the tests were carried out at the atmospheric air pressure, $\sigma_{vnet} = \sigma_v$.

164 ***Evaluation of Compressibility in MSL Tests***

165 A comparison of the normalised compression curves for Sheppey LC and the natural LC from
 166 Unit C (block sample retrieved from 5–10 m depth) of the Heathrow Terminal 5 site (T5)
 167 (Gasparre 2005) is shown in Fig. 3. The curves exhibited very similar characteristics with almost
 168 equal compression and swelling indices. The specimen from T5, however, is less compressible
 169 than the Sheppey specimen, mainly due to its lower plasticity index ($I_p = 37\%$) and initial water
 170 content ($w_0 = 24\%$). Moreover, the change in loading pattern, which was aimed at reducing the
 171 effects of sudden loading and subsequent damages to the soil structure, did not have a notable
 172 influence on the obtained compression curves. The only exception was the MSLis32-5 curve
 173 which was slightly shifted to the right, and exhibited lower compressibility which could be due to
 174 a lower S_r of the specimen at the start of the test. Furthermore, the highly structured nature of the
 175 specimens resulted in high C_s values. Similar observations were also reported by Gasparre (2005)
 176 for LC samples retrieved from T5. Average C_c and C_s values of respectively 0.218 and 0.096 were
 177 obtained from the compression tests on intact specimens having an average initial void ratio of e_0
 178 $= 0.85$ and initial water content of $w_0 = 32\%$.

179

180 Fig. 4 presents the results of MSL compression tests carried out on reconstituted specimens. It is
181 seen that with an increase of w_0 , the compressibility of the specimens is increased. Average C_c and
182 C_s values of respectively 0.383 and 0.125 were obtained from the compression tests on
183 reconstituted specimens having an average initial void ratio of 0.93 and initial water content of
184 39%. For specimens with $w_0 = 43\%$, the average C_c and C_s values of respectively 0.408 and 0.133
185 were obtained. Similar C_c values of 0.41 to 0.51 were reported by [Sorensen \(2006\)](#) from isotropic
186 compression and oedometer tests on reconstituted LC from T5. Similar to intact specimens, the
187 reconstituted compression curves of Sheppey and T5 LC were also compared. The reconstituted
188 Sheppey specimen exhibits less compressibility in comparison with the reconstituted T5 specimen.
189 This behaviour could be attributed to the modified PSD of the reconstituted Sheppey specimens
190 and the presence of sand-sized aggregates that resulted in an increased resistance against
191 compression.

192 To further investigate the effect of soil structure on the compressibility of Sheppey LC, a set of
193 three MSL oedometer tests were carried out on LQU specimens. A comparison of compression
194 curves for intact, reconstituted, and LQU specimens is shown in Fig. 5. The compression curve of
195 the LQU specimen with partly destroyed structure lies in between the compression curves of intact
196 and reconstituted specimens. The curve is more similar to the reconstituted compression curve,
197 highlighting the greater influence of soil structure than the initial water content on the
198 compressibility of stiff LC.

199 Fig. 6 presents the normalised compression curves for unsaturated reconstituted specimens. As it
200 can be seen, suction influences the shape and location of the compression curves. Increase in
201 suction level results in a decrease in overall compressibility of the specimens. Furthermore,
202 increase in suction results in an increase in yield vertical net stress (σ_p), a phenomenon known as
203 suction hardening ([Wheeler and Sivakumar, 1995](#)). The obtained data allows for defining the locus

204 of the yield points in suction-net mean stress plane known as Loading-Collapse yield curve in
205 Barcelona Basic Model (BBM) proposed by [Alonso et al. \(1990\)](#).

206 Fig. 7 presents the variation of pore-water pressure (u_w) during loading and unloading stages for
207 specimens MSLru37, MSLLru36, MSLru35 and MSLru28. Figs. 7(a) to 7(d) show an
208 instantaneous increase in u_w (decrease in suction) followed by a gradual pressure equalisation at
209 each loading stage. Moreover, for all loading stages, a suction state was preserved within the
210 specimens, confirming that no water had been expelled, and hence, the condition of constant water
211 content was recognised throughout the experiments. Similarly, instantaneous decrease in u_w
212 (increase in suction) followed by a pressure stabilisation was observed at each unloading stage.
213 Unlike the assumption of pore-fluid incompressibility in saturated consolidation theory, the pore-
214 fluid, being formed of gas (typically air) and liquid (typically water), is considered compressible
215 during consolidation of unsaturated clays. Therefore, during the course of compression, with a
216 decrease in air volume, the S_r is increased, this is mainly due to the reduction in void ratio of the
217 specimen. The decrease in suction observed at the end of the unsaturated MSL tests can be,
218 therefore, explained by the increase in S_r of the specimen.

219 Figs. 7(e) to 7(h) present the variation of suction with vertical stress changes ($ds/d\sigma$), once
220 equilibrium has been reached. As it can be seen on the graphs, suction is decreased during loading
221 and then increased by unloading. For vertical stresses up to 400 kPa (200 kPa for MSLru28), a
222 linear relationship between changes in suction and applied vertical stress was observed. Variation
223 of suction with vertical stresses higher than 400 kPa (200 kPa for MSLru28) appears to be almost
224 constant during both loading and unloading stages. The slopes obtained during loading were very
225 close and varied between -0.30 and -0.34. Except for the MSLru28 specimen, the slopes obtained
226 during unloading were also close and varied between -0.02 and -0.08. MSLru28 exhibited a higher
227 slope in unloading (-0.86) than loading (-0.30). For natural clays, the slopes obtained during the
228 unloading stage can be used for estimation of suction changes during sampling and release of

229 stresses (Delage et al. 2007). Although the experiments were performed on reconstituted samples,
 230 the obtained results clearly confirmed the importance of suction and suction release, in particular
 231 in stiff clays such as LC, even though it appears that suction changes during unloading for
 232 specimens with low initial suctions ($< \sim 500$ kPa) is not significant.

233 Further inspection of Figs. 7(a) to 7(d) reveals a slight increase in equalised suction at the early
 234 stages of loading (e.g. at $\sigma_v = 89$ kPa) for MSLru37, MSLru36, and MSLru35 specimens. A
 235 possible reason for such observation is that under constant water content conditions, the change in
 236 pore-water pressure (Δu) is expressed as;

$$(2) \quad \Delta u = B \times \Delta \sigma_v + \Delta u_d$$

237 Where B is the Skempton B value ($\Delta u / \Delta \sigma_v$) and Δu_d is the excess pore-water pressure accounted
 238 for a possible dilation within the aggregates. This dilation component (Δu_d) would be negative,
 239 therefore it may subdue the overall increase in Δu caused by $\Delta \sigma_v$. Therefore, it may be expected
 240 to see an increase in suction and hence, reduction in the overall B value at the early stages of
 241 compression under undrained conditions. Evolution of B value with vertical net stress during the
 242 loading and unloading stages is shown in Fig. 8. The fact that the B value is notably high at the
 243 early stages of loading might be due the high water content of the soil paste placed on the tip of
 244 HCT to ensure intimate contact between the porous filter and surrounding soil.

245 ***Stress-Dependent Response in MSL Tests***

246 Compressibility of intact and reconstituted clays can be evaluated from the variation of the slope
 247 of compression curve with vertical effective stress (σ'_v). The slope of compression curve (m_c) at
 248 each loading increment is calculated as $\Delta e / \Delta \log \sigma'_v$. The saturated yield vertical net stress (σ'_p)
 249 was determined as the intersection of the best fitted lines to the pseudo-elastic and plastic sections
 250 of the compression curve. For $\sigma'_v < \sigma'_p$, the calculated values represent the slope of the reloading
 251 line (i.e. C_r), and for $\sigma'_v > \sigma'_p$, the calculated values represent the slope of normal compression line

252 (i.e. C_c). Fig. 9 presents the relationship between m_c and normalised stress σ'_v/σ'_p for saturated
 253 intact, reconstituted, and LQU specimens. As it can be seen, change in the loading pattern (dotted
 254 lines) does not have a significant influence on the C_r and C_c values for intact specimens. Prior to
 255 the yield stress, the C_r values increase slightly. Following σ'_p , the values of C_c increase gradually
 256 until reaching a peak value around (8-10) σ'_p , after which, a gradual decrease in compressibility is
 257 observed. Unlike soft clays that exhibit a sudden increase of C_c in post yield region due to
 258 structural collapse (see for example [Mataic et al. 2016](#)), the process of destructuration in stiff LC
 259 appears to be continuous and follows an almost linear trend until reaching the peak value. In soft
 260 clays the peak value falls in a range of (2-3) σ'_p (e.g. [Karstunen and Yin 2010](#); [Mataic et al. 2016](#)),
 261 whereas for stiff LC this range is observed to extend to (8-10) σ'_p (see Fig. 9). Similar to intact
 262 specimens, the slope of reloading line for reconstituted specimens increases slightly prior to σ'_p .
 263 Increase in slope of reloading line for specimens with $w_0 = 43\%$ is reasonably higher than the
 264 specimens with $w_0 = 39\%$ given the higher water content that results in higher compressibility.
 265 The slope of compression curve in normal consolidation (NC) region increases dramatically to a
 266 peak value at stress levels between (3-4) σ'_p , at which it starts to decrease slowly. In soft clays,
 267 higher m_c values for intact specimens is typically observed in comparison with the reconstituted
 268 specimens, mainly due to the destructuration phenomenon that results in dramatic increase of C_c
 269 values in post yield region. However, as explained earlier, in stiff LC, degradation of inter-particle
 270 bonds (destructuration) does not occur suddenly and typically takes place gradually with increase
 271 in stress level. In overconsolidated (OC) region, the C_r values for LQU specimens increase at the
 272 same rate as the reconstituted specimens. However, in post yield region, the rate of increase in C_c
 273 for LQU specimens is lower than that of reconstituted specimens, this is in part, due to the lower
 274 w_0 and the presence of inter-particle bonds that result in reduction of compressibility. The
 275 maximum value of C_c for LQU specimens occurs in a range of (6-8) σ'_p .

276

277 Fig. 10 presents variation of the C_{ae} with normalised stress σ'_v/σ'_p for intact, reconstituted, and
 278 LQU specimens. It is observed that for doubling vertical stress method (dotted lines), C_{ae} increases
 279 gradually with stress level up to (3-4) σ'_p , at which it starts to increase dramatically to a peak value
 280 at stress levels in a range of (6-7) σ'_p . This behaviour can be attributed to the structural damage to
 281 the specimen during sudden loading at high stress levels. After the peak value, C_{ae} decreases
 282 dramatically. For specimens that the vertical stresses were applied in an unconventional way
 283 (continuous lines) following the pattern described in Table 2, it is observed that C_{ae} increases
 284 gradually with stress level up to (8-11) σ'_p , at which it starts to decrease. This unconventional
 285 loading method, therefore, appears to produce more reliable results although it involves more
 286 loading stages and hence, requires more time to complete. The maximum value of C_{ae} falls
 287 approximately in the range of 0.007 – 0.008 and 0.005 – 0.006 respectively for conventionally and
 288 unconventionally loaded intact specimens. For reconstituted specimens with $w_0 = 39\%$, C_{ae}
 289 increases slowly at stress levels prior to σ'_p . For stresses beyond yield stress, C_{ae} increases at a
 290 higher rate until reaching a peak value at stress levels in a range of (6-7) σ'_p at which it starts to
 291 decrease. For specimens with higher initial water content ($w_0 = 43\%$), variation of C_{ae} with
 292 normalised stress is slightly different, with C_{ae} increasing dramatically in OC region and then
 293 increasing gradually in NC region to a peak value at stress levels in a range of (3-4) σ'_p where a
 294 gradual reduction of C_{ae} values is observed. The maximum value of C_{ae} falls approximately in the
 295 range of 0.012 – 0.013 for all tested reconstituted specimens. This range is comparable with the
 296 average value of $C_{ae} = 0.016$ reported by [Sorensen \(2006\)](#) for reconstituted T5 LC.

297 Unlike natural soft clays which typically exhibit higher creep than their corresponding
 298 reconstituted specimens, stiff LC exhibits significantly less creep in comparison with the
 299 corresponding reconstituted specimens. This, on the one hand, can be attributed to the more
 300 compact nature of stiff clays (low initial void ratio) that results in reduced particles freedom for
 301 rearrangement under sustained σ'_v , and on the other hand, to the low w_0 of the intact specimens
 302 and presence of localised unsaturated pockets with sustainable water menisci developed at inter-

303 particle contacts preventing orientation and rearrangement of particles into a more packed state.
 304 In soft clays, the C_{ae} values for intact specimens essentially converge with intrinsic C_{ae} of the
 305 reconstituted specimens at high stress levels associated with the completely destroyed inter-
 306 particle bonds and rearranged fabric (Mataic et al. 2016). Indeed, much higher stress levels are
 307 required to observe such behaviour for stiff clays. For LQU specimens, it is observed that C_{ae}
 308 increases gradually with stress level up to (4-5) σ'_p , at which it starts to decrease. The response of
 309 LQU specimens is more similar to that of reconstituted ones, highlighting the effect of soil
 310 structure on creep strains.

311
 312 The ratio of $\alpha = C_{ae}/C_c$ in clays has been the subject of numerous studies in the past. Although
 313 early researchers such as Mesri and Godlewski (1977) and Mesri and Castro (1987) proposed
 314 constant values for α , recent experimental studies (e.g. Yin et al. 2011; Mataic et al. 2016) have
 315 demonstrated stress-dependency of α for soft clays. In order to examine the applicability of either
 316 of these two hypotheses for stiff Sheppey LC, the ratio α was investigated. Fig. 11 presents
 317 variation of C_{ae}/m_c ratio with normalised stress σ'_v/σ'_p for saturated intact, reconstituted, and LQU
 318 specimens. Unlike natural soft clays that exhibit a sudden increase to a peak value in post yield
 319 region due to destructuration phenomenon (Mesri and Castro 1987; Karstunen and Yin 2010;
 320 Mataic et al. 2016), variation of C_{ae}/m_c ratio with normalised stress for intact specimens does not
 321 present such trends. At lower stress levels (i.e. OC region), the C_{ae}/C_r ratio is considerably
 322 scattered. In NC region, the C_{ae}/C_c ratio decreases gradually with stress level. The values of α fall
 323 approximately in a range of 0.015 – 0.045. Moreover, the values of α for conventionally loaded
 324 specimens are generally greater than those of unconventionally loaded specimens (dotted lines).
 325 The less scattered values of α for unconventionally loaded specimens in post yield region can
 326 further approve the suitability of this loading method for investigating interrelation of compression
 327 and creep indices in stiff clays. Similar to intact specimens, the C_{ae}/C_r ratio for reconstituted
 328 specimens is considerably scattered at lower stress levels (i.e. OC region). However, in NC region,

329 the C_{ae}/C_c values are less scattered and decrease gradually to finally converge at the constant
 330 average value of 0.024. Moreover, the values of α in post yield region are in general smaller for
 331 intact specimens than reconstituted ones given lower C_c and C_{ae} values observed for intact
 332 specimens (see Figs. 9 and 10). In soft clays, the C_{ae}/C_c values essentially converge at a constant
 333 value corresponding to that of the reconstituted specimens. This is justified based on the principle
 334 that at high stress levels, all inter-particle bonds are destroyed and the post yield compression
 335 curve of a natural clay merges with the intrinsic compression line (ICL) associated with the
 336 corresponding reconstituted specimen. In soft clays, convergence of C_{ae}/C_c values for intact and
 337 reconstituted specimens may occur at stress levels in a range of (10-20) σ'_p due to the soft nature
 338 and high degree of destructuration in these materials. However, a much higher stress level may be
 339 required for degradation of inter-particle bonds in stiff clays such as LC. Applying such high
 340 stresses may not be typically possible using the conventional dead-weight loading method in
 341 oedometer apparatuses. Inspection of the results for LQU specimens reveals that, except for the
 342 MSLis32-7* specimen, the ratio of α for LQU specimens exhibits a peak value at stress levels in
 343 a range of (4-5) σ'_p , at which it starts to decrease towards the values of α ratio of the reconstituted
 344 specimens. In conclusion, it is clear that the C_{ae}/C_c ratio is stress-dependent and varies with the
 345 effective stresses. Therefore, the hypothesis of constant C_{ae}/C_c ratio is not applicable for the tested
 346 material.

347 ***Suction-Dependent Response in MSL Tests***

348 Fig. 12 presents the relationship between the slope of unsaturated compression curve ($m'_c =$
 349 $\Delta e/\Delta \log \sigma_{vnet}$) and vertical net stress (σ_{vnet}) for unsaturated reconstituted specimens. Similar to
 350 saturated reconstituted specimens (see Fig. 9), the slope of compression curves, calculated for each
 351 load increment, exhibits stress-dependency and increases with increase in σ_{vnet} . However, unlike
 352 the saturated specimens, a peak value, after which the m'_c is decreased, is not apparent. Moreover,
 353 it is clearly shown that increase in suction results in decrease of the m'_c values. To further
 354 investigate this phenomenon, the values of C_s and C_c for each test were plotted against the initial

355 suction of the specimen (Fig. 13). It is clearly observed that the C_c values decrease with increase
356 in suction. The C_s values also decrease with increase of suction and follow an approximately linear
357 trend. The latter observation contradicts with the statement of [Sivakumar \(1993\)](#) that the gradient
358 of swelling lines are almost independent of suction level. The former observation also contradicts
359 with the results of suction-controlled oedometer tests on compacted LC, performed by [Monroy et
360 al. \(2008\)](#), who reported an increase in C_c values with increase in soil suction. The reason behind
361 such contradiction can be attributed to the sample preparation method and the initial conditions of
362 the test specimens. [Monroy et al. \(2008\)](#) prepared the samples by static compaction to an initial
363 suction of 1000 kPa, and then decreased the suction by hydrating the samples to different
364 equilibrium suctions (zero, 120, and 405 kPa). Therefore, the observed differences in
365 compressibility responses can be explained, in one hand, by the differences in mechanical response
366 of compacted and reconstituted samples, and in other hand, by the initial hydraulic states of the
367 two samples positioned respectively on the main drying (reconstituted) and main wetting
368 (compacted) curves of the SWRC.

369 The compression index as a function of suction has been the subject of a long-term dispute among
370 the researchers. Different approaches, as discussed in [Zhou et al. \(2012\)](#), have been proposed to
371 overcome the problems associated with assuming C_c as a function of suction. Among which, the
372 assumption of C_c as a function of S_r appears to be a more logical approach which also produces a
373 better match to the experimental data when used in constitutive models ([Zhou et al. 2012](#)). This
374 approach implies that C_c increases with increase in S_r . In other words, it is possible to saturate an
375 unsaturated soil by compressing it under constant suction. In fact, in constant suction compression,
376 increase in S_r as a result of reduction in void ratio, can increase the compressibility of the soil due
377 to the stress-induced collapse of macro-pores ([Zhou et al. 2012](#)). Based on this approach, increase
378 of C_c is small at low stresses, and becomes larger at intermediate stress levels until finally equalises
379 the C_c value corresponding to the saturated condition. This behaviour is clearly shown in Fig. 12.
380 The only difference is that the C_c values of unsaturated specimens do not essentially converge with

381 the values of their saturated condition. Higher applied total stresses might be required to observe
 382 such convergences. Moreover, as shown in Fig. 7, in drained compression tests carried out here,
 383 suction evolves throughout the experiment and ends up with a lower value than the s_0 at the start
 384 of the test. Therefore, the conditions of constant suction tests, typical of suction-controlled
 385 oedometer tests, are not met here. Essentially, for the material tested here, it can be concluded that
 386 the slope of compression curve decreases with increase of soil suction.

387 Fig. 14 presents variation of the C_{ae} with vertical net stress (σ_{vnet}) for unsaturated reconstituted
 388 specimens. Similar to saturated reconstituted specimens (see Fig. 10), the C_{ae} , calculated for each
 389 load increment, exhibits stress-dependency and increases with increase in σ_{vnet} . However, unlike
 390 the saturated specimens, a peak value, after which the C_{ae} is decreased, is not apparent. In a rough
 391 estimation, for specimens with s_0 of 362, 1405, 1907, and 21000 kPa, the maximum value of creep
 392 index appears to occur at 710, 500, 500, and 400 kPa vertical total stress respectively. Furthermore,
 393 increase of C_{ae} is small at low stress levels (< 200 kPa), and becomes larger at higher stress levels.
 394 Moreover, it is clearly observed that increase in suction results in a decrease of the C_{ae} values.
 395 With development of partial saturation state in the specimen during drying, the u_w becomes
 396 negative at the back of the generated water menisci at the inter-particle contacts, applying tensile
 397 pressure to the soil grains. The additional attractive forces exerted from the water menisci and
 398 contractile skin, contribute to the reduction of particles' freedom for rearrangement under
 399 sustained effective stress. The rate and magnitude of volumetric creep strains (ϵ_v^{cr}) are, therefore,
 400 decreased with the increase in soil suction.

401 Fig. 15 presents the variation of C_{ae}/m'_c ratio with vertical net stress for unsaturated reconstituted
 402 specimens. At low stress levels (< 200 kPa), the values of C_{ae}/m'_c decrease with increase in σ_{vnet} .
 403 However, at higher stress levels, the values of C_{ae}/m'_c are scattered and do not follow a clear trend.
 404 In a rough estimation, the values of $\alpha = C_{ae}/C_c$ could approximately be considered constant with
 405 increase in stress level. Excluding the MSLru15 specimen, the values of α obtained for unsaturated
 406 conditions appear to fall within a range of 0.023 – 0.030. Note that in saturated conditions, the

407 values of α decrease gradually to finally converge at a constant value of 0.024, whereas in
 408 unsaturated conditions a clear trend and/or convergence is not observed.

409 ***Evaluation of α Ratio for Sheppey London Clay***

410 Table 4 summarises the stress ranges at which the maximum values of C_c , C_{ae} , and α occur for
 411 both intact and reconstituted specimens. The range and average values of α ratio obtained from
 412 different sets of experiments are also presented. The results indicate that for conventionally loaded
 413 intact specimens as well as reconstituted specimens with $w_0 = 0.39$, the maximum values of C_c
 414 and C_{ae} do not occur at the same stress level. However, for unconventionally loaded intact
 415 specimens as well as reconstituted specimens with $w_0 = 0.43$, C_c and C_{ae} reach the peak value at
 416 the same stress levels synchronously. The latter finding is in contradiction with the limited
 417 available observations reported in the literature for soft clays (see [Mataic et al. 2016](#)). The
 418 maximum values of α occur at stress levels in a range of (1-2) σ'_p , for both intact and reconstituted
 419 specimens. For unsaturated specimens, a peak value for C_c , C_{ae} , and α was not apparent. For
 420 saturated intact specimens, the range of α values varies significantly. For conventionally loaded
 421 intact specimens, an average α value of 0.03 ± 0.02 can be approximated. However, for
 422 unconventionally loaded intact specimens, a lower approximate average α value of 0.02 ± 0.01 is
 423 obtained. According to the classification criterion defined by [Mesri et al. \(1994\)](#), Sheppey London
 424 Clay lies in the zone of shale or mudstone whose α value ranges from 0.02 to 0.04. For saturated
 425 and unsaturated reconstituted specimens, the ratio C_{ae}/C_c lies in a similar range of 0.023 – 0.037.
 426 Accordingly, an average value of 0.03 ± 0.01 can be approximated for the α ratio of saturated and
 427 unsaturated reconstituted specimens. The values of α for saturated LQU specimens fall in a range
 428 of 0.023 – 0.048, with the lower band value being equal to that of reconstituted specimens, and
 429 the upper band value, being similar to that of intact specimens.

430 ***Stress- and Suction-Dependent Response in SSL Tests***

431 Test results in this section are presented in plots of normalised void ratio e/e_p versus logarithm of
432 time, where e_p is the void ratio obtained 24 hours after the end of loading. The decision of
433 considering the results obtained after a period of 24 hours was made so as to ensure full dissipation
434 of u_{exc} , and also to allow for comparison between the results and define a criterion applicable to
435 all experiments. Similar approach was considered by Cui et al. (2009) for investigating time-
436 dependent behaviour of stiff Boom Clay.

437 Fig. 16 compares variation of the normalised void ratio e/e_p with logarithm of time for intact and
438 reconstituted specimens at different stress levels. For all specimens, higher volume changes were
439 observed with increase in σ_{vm} , indicating the stress-dependency of creep strains. The rate of change
440 in void ratio for all specimens was higher during the first 10 days of sustained loading, after which
441 it started to decrease. For intact and reconstituted specimens, the observed behaviour corresponds
442 to primary creep stage characterised as increasing creep strains at a decreasing strain-rate.
443 Furthermore, the creep rate and magnitude appears to be, in general, lower for intact specimens
444 than the reconstituted ones, this being, in part, due to the low w_0 of the intact specimens. Soil
445 structure, i.e. fabric anisotropy and inter-particle bonding, also plays a significant role in
446 controlling deformations. The process of destructuration during single-stage loading, and whether
447 the inter-particle bonds were fully or partly destroyed, is not, however, clearly identified.
448 Moreover, at the same stress level, the rate and magnitude of change in void ratio for reconstituted
449 specimens with higher initial water contents ($w_0 = 0.43$) were found to be higher. In the absence
450 of inter-particle bonds, the water content of the specimens appears to control the rate and
451 magnitude of creep strains.

452 Graphs of Fig. 17 present the variation of normalised void ratio e/e_p with logarithm of time for
453 specimens having different initial water contents (and therefore different suctions), and subjected
454 to similar vertical stresses. It is clearly observed that at the same vertical stress level, decrease in

455 w_0 (or increase in s_0) results in a decrease in the rate and magnitude of ε_v^{cr} . Unlike saturated soils,
456 the water phase in partially-saturated soils is discontinuous. The generated water menisci between
457 the soil particles hold the grains together and the soil particles are held together by the tensile
458 forces at the solid-water interface. During creep under constant effective stress, the under-tension
459 water menisci resist against rearrangement and orientation of the clay particles.

460 Similar to saturated conditions (Fig. 16), creep behaviour in unsaturated conditions appears to be
461 stress-dependent. However, effect of increase in σ_{vm} is more pronounced during the final stages of
462 the unsaturated tests. For specimens SLLru28-444 and SLLru28-355 with $s_0 = 1405$ kPa, the
463 volume change response appears to be fairly similar, indicating the predominant effect of soil
464 suction in controlling creep deformations. Similar behaviour is also observed for SLLru26-222
465 and SLLru26-178 specimens with $s_0 = 1907$ kPa, further supporting this hypothesis. The
466 predominant effect of suction is not, however, apparent for specimens with lower initial suctions.
467 Similar to MSL tests, an instantaneous increase in u_w (decrease in suction) followed by a gradual
468 pressure equalisation at each loading stage was observed. Moreover, for all loading stages, a
469 suction state was preserved within the specimens, confirming that no water was expelled, and
470 hence, the condition of constant water content was recognised throughout the loading stage. Fig.
471 18 presents the results of monitoring suction evolutions during the creep stage of the tests. It is
472 observed that suction is decreased with time for all of the test specimens. In fact, with increase in
473 creep strains at constant water content, total volume is decreased resulting in an increase in the S_r ,
474 which in turn, leads to a decrease in soil suction. This is, however, a possible mechanism, and the
475 observed decrease in suction might be due to other factors influencing the HCTs measurements.
476 However, if this is the case, keeping the soil suction constant during a constant suction creep test
477 may not be ideal, as this may require a change (reduction) in S_r of the specimen, and hence,
478 artificially development of creep strains.

479

480 **Conclusions**

481 Results of a set of MSL and SSL oedometer tests performed on Sheppey London Clay specimens
 482 under different conditions of saturated intact, saturated reconstituted, and unsaturated
 483 reconstituted were presented. The following conclusions can be drawn;

- 484 - The change in loading pattern, which was aimed at reducing the effects of sudden loading
 485 and subsequent damages to the soil structure during MSL tests, does not have a notable
 486 influence on the obtained compression curves and the C_r and C_c values for intact
 487 specimens; however, it leads to lower C_{ae}/C_c values than the conventionally loaded
 488 specimens.
- 489 - Unlike soft clays that exhibit a sudden increase of C_c in the post yield region due to
 490 structural collapse, the process of destructuration in stiff LC appears to be continuous and
 491 follows an almost linear trend.
- 492 - Unlike natural soft clays which typically exhibit higher creep than their corresponding
 493 reconstituted specimens, stiff LC exhibits significantly less creep in comparison with the
 494 corresponding reconstituted specimens. This, on the one hand, can be attributed to the more
 495 compact nature of stiff clays (low e_0), and on the other hand, to the low w_0 of the intact
 496 specimens.
- 497 - Generally, for Sheppey LC, increase in suction results in a decrease in the slope of
 498 compression curve (m'_c) and the C_{ae} values, and an increase in σ_p .
- 499 - According to the classification criterion defined by [Mesri et al. \(1994\)](#), Sheppey LC is
 500 categorised as shale or mudstone whose α value ranges from 0.02 to 0.04. The $\alpha = C_{ae}/C_c$
 501 ratio for Sheppey LC is stress- and suction-dependent, and therefore cannot be considered
 502 as a constant value. However, as a rough estimation, an average value of 0.03 ± 0.01 can
 503 be approximated for the α ratio of saturated and unsaturated reconstituted specimens.

- 504 - During SSL tests, at the same vertical stress level, decrease in w_0 (or increase in s_0) results
505 in a decrease in the rate and magnitude of ε_v^{cr} . Moreover, at the same s_0 , increase in applied
506 vertical stress leads to an increase in the ε_v^{cr} .
- 507 - The volume change of specimens with high s_0 during SSL tests appears to be
508 predominantly controlled by the state of suction stress rather than the applied vertical
509 stress.
- 510 - During long-term creep tests at constant water content, a decrease in soil suction monitored
511 by HCTs can be attributed to an increase in S_r of the specimen with decrease in total volume
512 during creep. If this holds true, long-term creep tests where suction is artificially kept
513 constant may not be ideal and the observed creep strains may not be solely attributed to
514 the applied total vertical stress.
- 515 - Further investigations and more test results over a wider range of soil suction and applied
516 vertical stress levels are required to validate the observed time-dependent response for the
517 tested soil.
- 518

519 **References**

- 520 Alonso, E.E., Gens, A. and Josa, A. 1990. A constitutive model for partially saturated soils.
521 *Géotechnique*, **40**(3): 405–430. doi: 10.1680/geot.1990.40.3.405.
- 522 Bagheri, M., Rezania, M. and Mousavi Nezhad, M. 2015. An experimental study of the initial
523 volumetric strain rate effect on the creep behaviour of reconstituted clays. IOP Conference
524 Series: Earth and Environmental Science, **26**(1): 012034.
- 525 Bagheri, M., Rezania, M. and Mousavi Nezhad, M. 2018. Cavitation in high-capacity
526 tensiometers: effect of water reservoir surface roughness. *Geotechnical Research*, **5**(2):
527 81–95. doi: 10.1680/jgere.17.00016.
- 528 Bagheri, M., Mousavi Nezhad, M., and Rezania, M. 2019a. A CRS oedometer cell for unsaturated
529 and non-isothermal tests. *Geotechnical Testing Journal*, **43**(1), in press. doi:
530 10.1520/GTJ20180204.
- 531 Bagheri, M., Rezania, M., and Mousavi Nezhad, M. 2019b. Rate-dependency and stress relaxation
532 of unsaturated clays, *International Journal of Geomechanics*, In Press.
- 533 Cui, Y.-J., Le, T.T., Tang, A.M., Delage, P. and Li, X.L. 2009. Investigating the time-dependent
534 behaviour of Boom clay under thermomechanical loading. *Géotechnique*, **59**(4): 319–329.
535 doi: 10.1680/geot.2009.59.4.319.
- 536 De Gennaro, V., Delage, P., Cui, Y.J., Schroeder, C. and Collin, F. 2003. Time-dependent
537 behavior of oil reservoir chalk: a multiphase approach. *Soils and Foundations*, **43**(4): 131–
538 147. doi: 10.3208/sandf.43.4_131.
- 539 De Gennaro, V., Sorgi, C. and Delage, P. 2005. Air-water interaction and time dependent
540 compressibility of a subterranean quarry chalk. Paper presented in Symposium Post
541 Mining, Nancy, France, pp. 1–12.
- 542 Delage, P., Le, T.T., Tang, A.M., Cui, Y.J. and Li, X.L. 2007. Suction effects in deep Boom Clay
543 block samples. *Géotechnique*, **57**(2): 239–244. doi: 10.1680/geot.2007.57.2.239.

- 544 Fredlund, D.G. and Xing, A. 1994. Equations for the soil-water characteristic curve. Canadian
545 Geotechnical Journal, **31**(3): 521–532. doi: 10.1139/t94-061.
- 546 Fredlund, D.G. 2006. Unsaturated soil mechanics in engineering practice, Journal of Geotechnical
547 and Geoenvironmental Engineering, **132**(3): 286–321. doi: 10.1061/(ASCE)1090-
548 0241(2006)132:3(286)
- 549 Gasparre, A. 2005. Advanced laboratory characterisation of London Clay. Ph.D. Thesis, University
550 of London.
- 551 Karstunen, M. and Yin, Z.-Y. 2010. Modelling time-dependent behaviour of Murro test
552 embankment. Géotechnique, **60**(10): 735–749. doi: 10.1680/geot.8.P.027.
- 553 Lai, X., Wang, S., Qin, H. and Liu, X. 2010. Unsaturated creep tests and empirical models for
554 sliding zone soils of Qianjiangping landslide in the Three Gorges. Journal of Rock
555 Mechanics and Geotechnical Engineering, **2**(2): 149–154. doi:
556 10.3724/SP.J.1235.2010.00149.
- 557 Li, J.Z., Peng, F.L. and Xu, L.S. 2009. One-dimensional viscous behavior of clay and its
558 constitutive modeling. International Journal of Geomechanics, **9**(2): 43–51. doi:
559 10.1061/(ASCE)1532-3641(2009)9:2(43).
- 560 Li, J.Z., Peng, F.L., Xu, L.S. and Tatsuoka, F. 2006. Viscous properties of clay with different
561 water content. Soil and rock behavior and modeling (GSP 150), ASCE, **194**: 55–61. doi:
562 10.1061/40862(194)6.
- 563 Li, J.-Z., Tatsuoka, F., Nishi, T. and Komoto, N. 2003. Viscous stress-strain behaviour of clay
564 under unloaded conditions. *In* Proceedings of the 3rd International Symposium on
565 Deformation Characteristics of Geomaterials: IS Lyon 03, Lyon, France, pp. 617–625.
- 566 Mataic, I., Wang, D. and Korkiala-Tanttu, L. 2016. Effect of destructuration on the compressibility
567 of Pernio clay in incremental loading oedometer tests. International Journal of
568 Geomechanics, **16**(1): 040150161. doi: 10.1061/(ASCE)GM.1943-5622.0000486.

- 569 Mesri, G. and Castro, A. 1987. C_u/C_c concept and K_0 during secondary compression. Journal of
570 Geotechnical Engineering, **113**(3): 230–247. doi: 10.1061/(ASCE)0733-
571 9410(1987)113:3(230).
- 572 Mesri, G. and Godlewski, P. M. 1977. Time and stress-compressibility interrelationship. Journal
573 of Geotechnical Engineering Division, American Society of Civil Engineeres, **103**(5):
574 417–430.
- 575 Mesri, G., Kwan, L.D.O., and Feng, W.T. 1994. Settlement of embankment on soft clays. *In*
576 Proceedings of the Conference on Vertical and Horizontal Deformations of Foundations
577 and Embankments: Part 2 (of 2), College Station, TX, USA, American Society of Civil
578 Engineers, GSP 1(40), pp. 8–56.
- 579 Mesri, G. 2009. Discussion of ‘Effects of friction and thickness on long-term consolidation
580 behavior of Osaka Bay clays’ by Watabe, Udaka, Kobayashi, Tabata & Emura 2008. Soils
581 and Foundation., **49**(5): 823–824.
- 582 Monroy, R., Zdravkovic, L. and Ridley, A.M. 2008. Volumetric behaviour of compacted London
583 Clay during wetting and loading. *In* Proceedings of the 1st European Conference on
584 Unsaturated Soils, E-UNSAT 2008, Durham, UK, pp. 315–320.
- 585 Nazer, N.S.M., and Tarantino, A. 2016. Creep response in shear of clayey geo-materials under
586 saturated and unsaturated conditions. *In* Proceedings of the 3rd European Conference on
587 Unsaturated Soils, E-UNSAT 2016, Paris, France, pp. 1–5.
- 588 Oldecop, L.A., and Alonso, E.E. 2007. Theoretical investigation of the time-dependnet behaviour
589 of rockfill. *Géotechnique*, **57**(3): 289–301. doi: 10.1680/geot.2007.57.3.289.
- 590 Pereira, J.M. and De Gennaro, V. 2010. On the time-dependent behaviour of unsaturated
591 geomaterials. *In* Proceedings of the 5th International Conference on Unsaturated Soils,
592 Barcelona, Spain, pp. 921–925.

- 593 Priol, G., De Gennaro, V., Delage, P. and Servant, T. 2007. Experimental investigation on the time
594 dependent behavior of a multiphase chalk. *In* Experimental unsaturated soil mechanics.
595 Edited by T. Schanz, Springer Proceedings Physics 112, pp. 161–167.
- 596 Rezania, M., Bagheri, M., Mousavi Nezhad, M. and Sivasithamparam, N. 2017. Creep analysis of
597 an earth embankment on soft soil deposit with and without PVD improvement. *Geotextiles
598 and Geomembranes* **45**(5): 537–547. doi: 10.1016/j.geotexmem.2017.07.004.
- 599 Sivakumar, V. 1993. A critical state framework for unsaturated soil. Ph.D. Thesis, University of
600 Sheffield, UK.
- 601 Sorensen, K.K. 2006. Influence of viscosity and ageing on the behaviour of clays. Ph.D. Thesis,
602 University College London.
- 603 Wheeler, S. J. and Sivakumar, V. 1995. An elasto-plastic critical state framework for unsaturated
604 soil. *Géotechnique*, **45**(1): 35–53. doi: 10.1680/geot.1995.45.1.35.
- 605 Yin, J.-H. and Feng, W.-Q. 2017. A new simplified method and its verification for calculation of
606 consolidation settlement of a clayey soil with creep. *Canadian Geotechnical Journal*, **54**(3):
607 333–347. doi: 10.1139/cgj-2015-0290.
- 608 Yin, Z.-Y., Karstunen, M., Chang, C.S., Koskinen, M. and Lojander, M. 2011. Modeling time-
609 dependent behavior of soft sensitive clay. *Journal of Geotechnical and Geoenvironmental
610 Engineering*, **137**(11): 1103–1113. doi: 10.1061/(ASCE)GT.1943-5606.0000527.
- 611 Zhou, A.N., Sheng, D., Sloan, S.W. and Gens, A. 2012. Interpretation of unsaturated soil
612 behaviour in the stress–saturation space, I: Volume change and water retention behaviour.
613 *Computers and Geotechnics*, **43**: 178–187. doi: 10.1016/j.compgeo.2012.04.010.
- 614
615

616 **List of Symbols**

- C_c = compression index in $e - \log \sigma'_v$ space
 C_r = reloading index in $e - \log \sigma'_v$ space
 C_s = swelling index in $e - \log \sigma'_v$ space
 C_{ae} = creep index with respect to e
 e = void ratio
 e_0 = initial void ratio
 e_i = instantaneous change in void ratio
 e_p = void ratio 24 hours after the end of loading in SSL tests
 G_s = specific gravity
 I_p = plasticity index
 k_v = coefficient of vertical permeability
 m'_c = slope of compression curve in $e - \log \sigma_v$ space for unsaturated conditions
 m_c = slope of compression curve in $e - \log \sigma'_v$ space for saturated conditions
 S_r = degree of saturation
 s = soil suction
 s_0 = initial suction
 t = time
 u_a = pore-air pressure
 u_{exc} = excess pore-water pressure
 u_w = pore-water pressure
 w = gravimetric water content
 w_0 = initial gravimetric water content
 w_L = liquid limit
 w_P = plastic limit
 α = represents the ratio C_{ae}/C_c
 β = represents the ratio e_i/e_p
 ε_v^{cr} = volumetric creep strain
 σ_p = yield vertical net stress in unsaturated states
 σ'_p = yield vertical net stress in saturated states
 σ_v = applied vertical total stress
 σ'_v = vertical effective stress
 σ_{vm} = maximum applied vertical stress
 σ_{vnet} = net normal stress

617

List of Tables

Table 1. Physical properties of Sheppey London Clay samples

Clay (%)	Silt (%)	Sand (%)	<i>in-situ</i> w (%)	w_p (%)	w_L (%)	G_s	k_v (m/s) at 20° C
64	34	2	29 – 35	19 – 24	70 – 78	2.67	2.5×10^{-10}

Table 2. Details of MSL tests

Test ID	Loading/unloading stresses (kPa)	w_0 (%)	s_0 (kPa)	σ_{vm} (kPa)	Test duration (days)	Test condition
MSLis32-1	22-44-89-178-355-710-1421-710-355-178-89	32		1421	11	Saturated
MSLis32-2	22-44-89-178-355-710-1421-710-355-178-89	32		1421	11	
MSLis32-3	22-44-89-178-355-710-1421-710-355-178-89	32		1421	11	
MSLis32-4	11-22-44-89-178-222-333-444-666-888-1110-1332-1110-888-666-444-333-222-178	32		1332	19	
MSLis32-5	11-22-44-89-178-222-333-444-666-888-1110-1332-1110-888-666-444-333-222-178	32		1332	19	
MSLis32-6	11-22-44-89-178-222-333-444-666-888-1110-1332-1110-888-666-444-333-222-178	32		1332	19	
MSLis32-7*	22-44-89-133-178-222-333-444-666-888-1110-888-666-444-333-222-178-133	32		1110	18	
MSLis32-8*	22-44-89-133-178-222-333-444-666-888-1110-888-666-444-333-222-178-133	32		1110	18	
MSLis32-9*	22-44-89-133-178-222-333-444-666-888-1110-888-666-444-333-222-178-133	32		1110	18	
MSLrs39-1	11-22-44-89-178-355-710-1421-710-355-178-44	39		1421	12	
MSLrs39-2	11-22-44-89-178-355-710-1421-710-355-178-44	39		1421	12	
MSLrs39-3	11-22-44-89-178-355-710-1421-710-355-178-44	39		1421	12	
MSLrs43-1	11-22-44-89-178-355-710-1421-710-355-178-44	43		1421	12	
MSLrs43-2	11-22-44-89-178-355-710-1421-710-355-178-44	43		1421	12	
MSLrs43-3	11-22-44-89-178-355-710-1421-710-355-178-44	43		1421	12	
MSLru37	22-44-89-178-355-710-1110-710-355-178-89-44-22-11	37	326	1111	14	Unsaturated
MSLru36	22-44-89-178-355-710-1110-710-355-178-89-44-22-11	36	433	1111	14	
MSLru35	22-44-89-178-355-710-1110-710-355-178-89-44-22-11	35	513	1111	14	
MSLru28	25-50-100-200-300-400-500-580-500-400-300-200-100-50-25	28	1405	605	15	
MSLru26	25-50-100-200-300-400-500-580-500-400-300-200-100-50-25	26	1907	605	15	
MSLru15	25-50-100-200-300-400-500-580-500-400-300-200-100-50-25	15	~21000	605	15	

r: reconstituted, i: intact, s: saturated, u: unsaturated, *: low-quality undisturbed
 The number before dash indicates initial water content and the number after dash indicates the test number.

Table 3. Details of SSL creep oedometer tests

Test ID	w_0 (%)	s_0 (kPa)	σ_{vm} (kPa)	Test duration (days)	Test conditions
SSLis32-178	32		178	37	Saturated
SSLis32-222	32		222	36	
SSLis32-355	32		355	36	
SSLis32-444	32		444	38	
SSLis32-666	32		666	38	
SSLrs39-178	39		178	60	
SSLrs39-222	39		222	68	
SSLrs39-355	39		355	68	
SSLrs39-444	39		444	46	
SSLrs39-666	39		666	46	
SSLrs43-355	43		355	94	Unsaturated
SSLrs43-444	43		444	94	
SSLru37-666	37	326	666	28	
SSLru37-444	37	326	444	29	
SSLru37-355	37	326	355	36	
SSLru36-666	36	433	666	28	
SSLru36-444	36	433	444	21	
SSLru36-355	36	433	355	34	
SSLru35-355	35	513	355	34	
SSLru35-222	35	513	222	34	
SSLru35-178	35	513	178	27	
SSLru28-666	28	1405	666	20	
SSLru28-444	28	1405	444	21	
SSLru28-355	28	1405	355	28	
SSLru26-222	26	1907	222	23	
SSLru26-178	26	1907	178	23	
The number after dash shows the σ_{vm} .					

Table 4. Stress ranges for maximum C_c , C_{ae} , and α parameters

Test ID	σ'_v / σ'_p or σ_v / σ_p			Range of α values	Average α
	$(C_c)_{\max}$	$(C_{ae})_{\max}$	$(\alpha)_{\max}$		
MSLis32-1					
MSLis32-2	8 – 10	6 – 7	1 – 2	0.015 – 0.046	0.031 ± 0.016
MSLis32-3					
MSLis32-4					
MSLis32-5	8 – 10	8 – 11	1 – 2	0.017 – 0.031	0.024 ± 0.007
MSLis32-6					
MSLis32-7*					
MSLis32-8*	6 – 8	4 – 5	4 – 5	0.023 – 0.048	0.036 ± 0.013
MSLis32-9*					
MSLrs39-1					
MSLrs39-2	3 – 4	6 – 7	1 – 2	0.022 – 0.037	0.03 ± 0.008
MSLrs39-3					
MSLrs43-1					
MSLrs43-2	3 – 4	3 – 4	1 – 2	0.024 – 0.036	0.03 ± 0.006
MSLrs43-3					
MSLru37					
MSLru28	3 – 4	2 – 5	NA	0.023 – 0.037	0.03 ± 0.007
MSLru26					
MSLru36					
MSLru35	NA	NA	NA	0.023 – 0.045	0.034 ± 0.011
MSLru15					

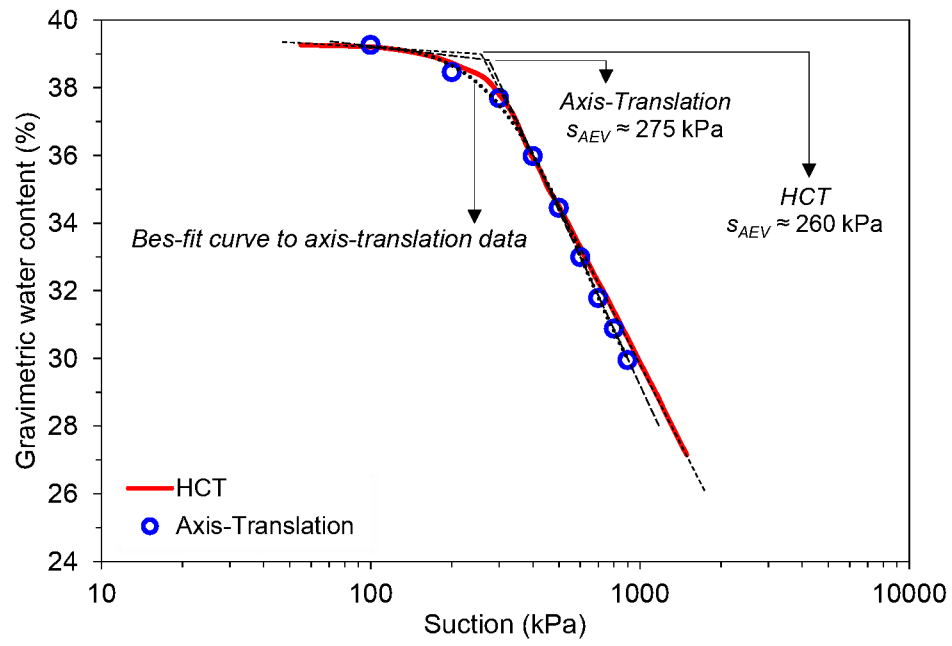


Fig. 1 SWRC determined for main drying path

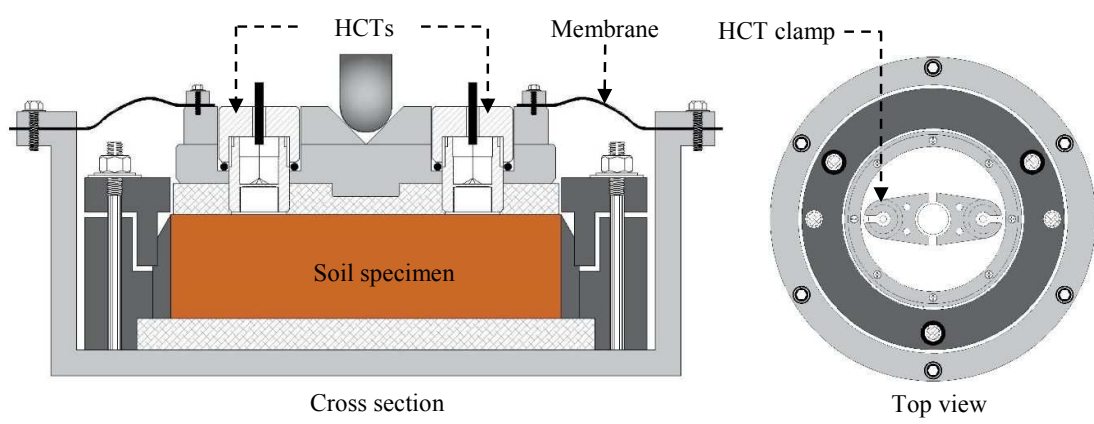


Fig. 2. Schematic diagram of the unsaturated oedometer cell

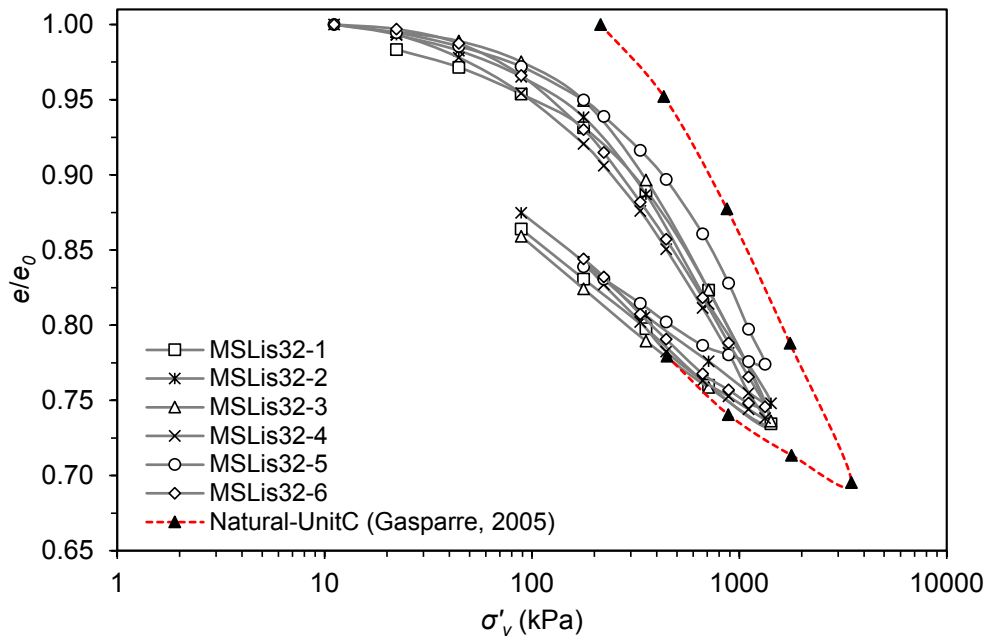


Fig. 3. Comparison of the compression curves for intact Sheppey LC and natural LC from Unit C of Heathrow T5 site

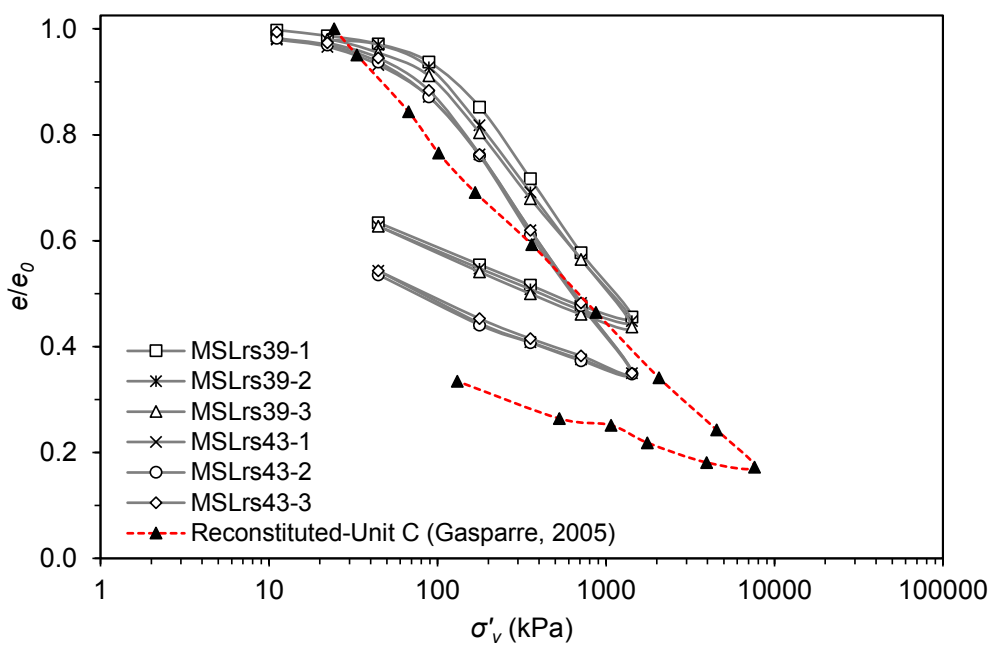


Fig. 4. Comparison of the compression curves for reconstituted Sheppey LC and natural LC from Unit C of Heathrow T5 site

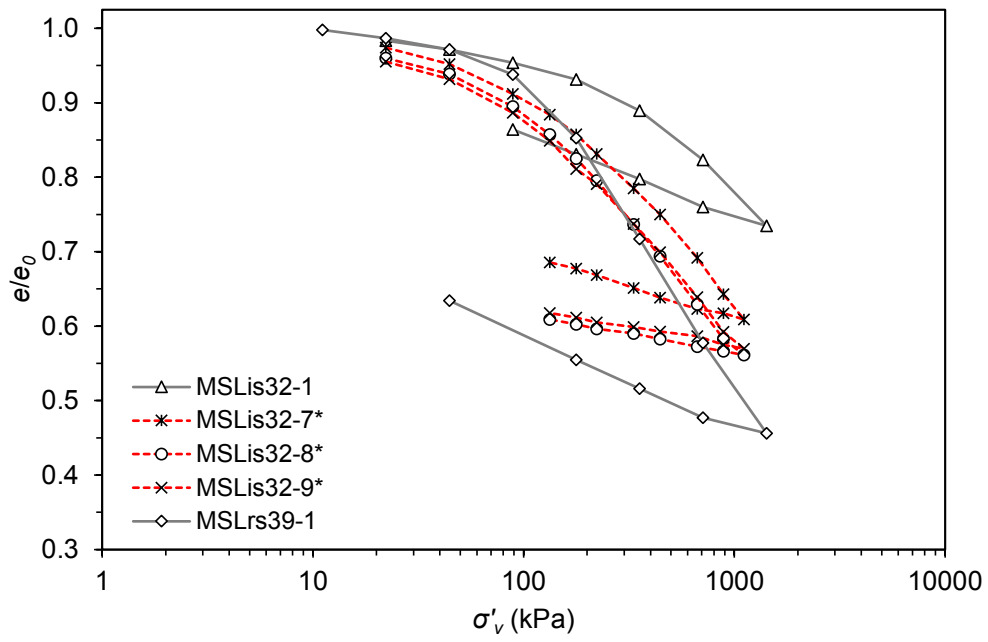


Fig. 5. Comparison of the compression curves for saturated intact, reconstituted, and LQU specimens

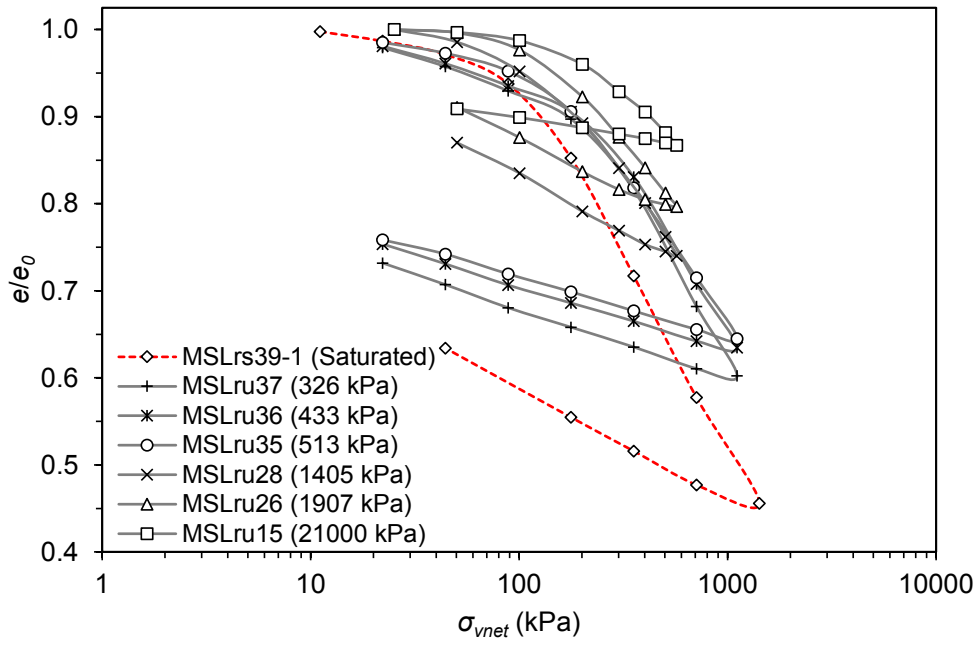


Fig. 6. Compression curves for unsaturated reconstituted specimens

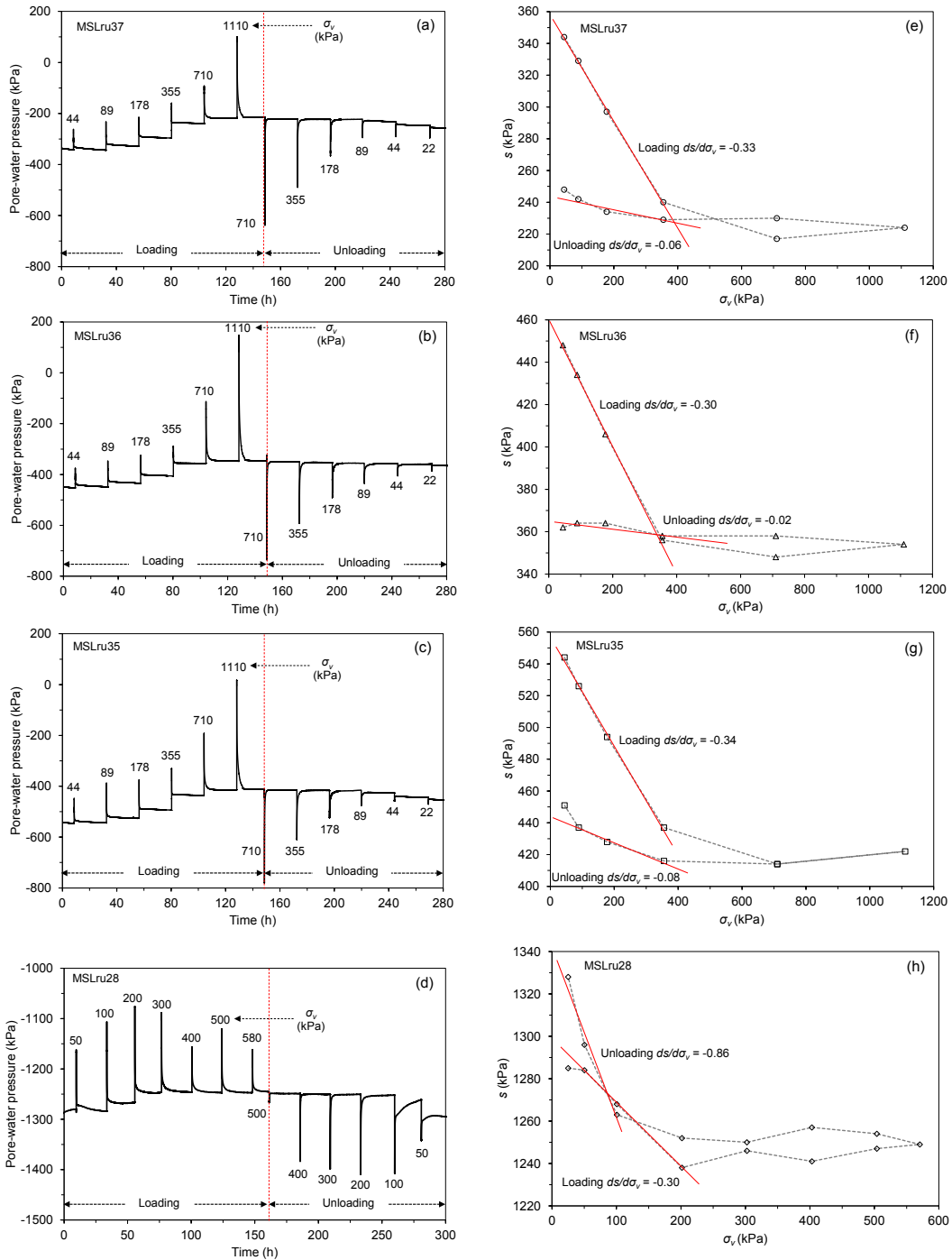


Fig. 7. Monitoring suction changes during step loading oedometer tests

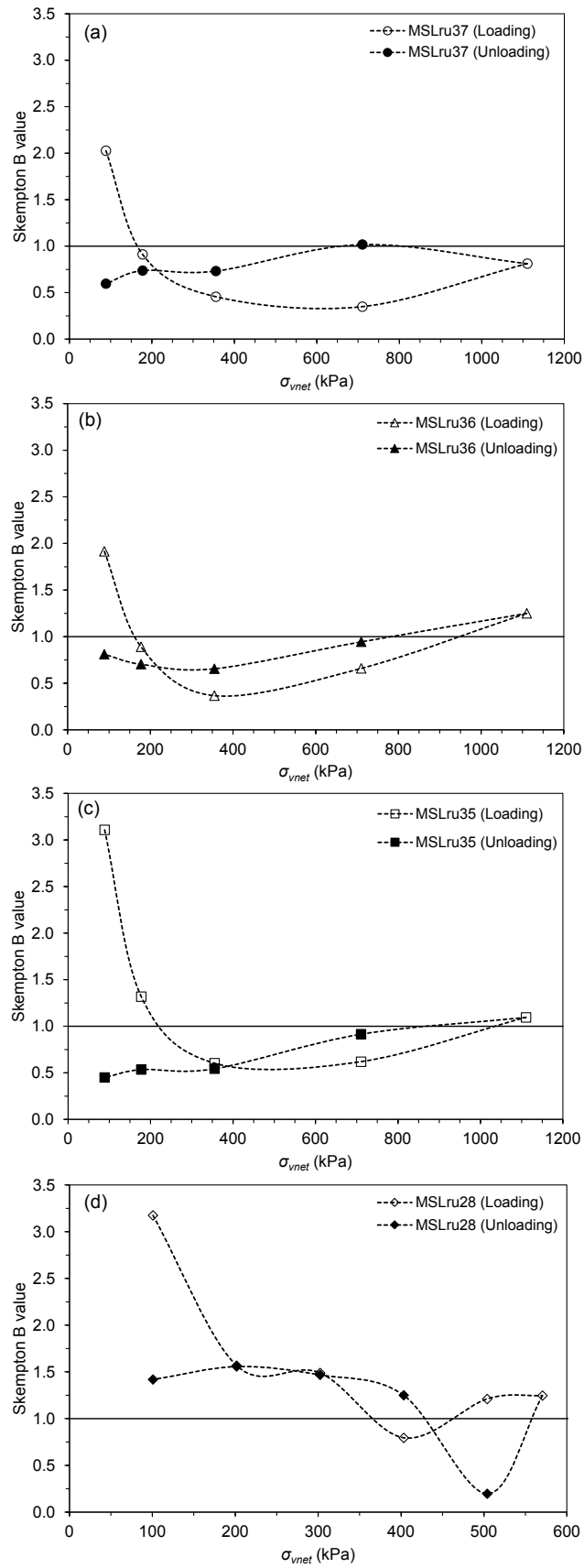


Fig. 8. Evolution of Skempton B value with vertical net stress

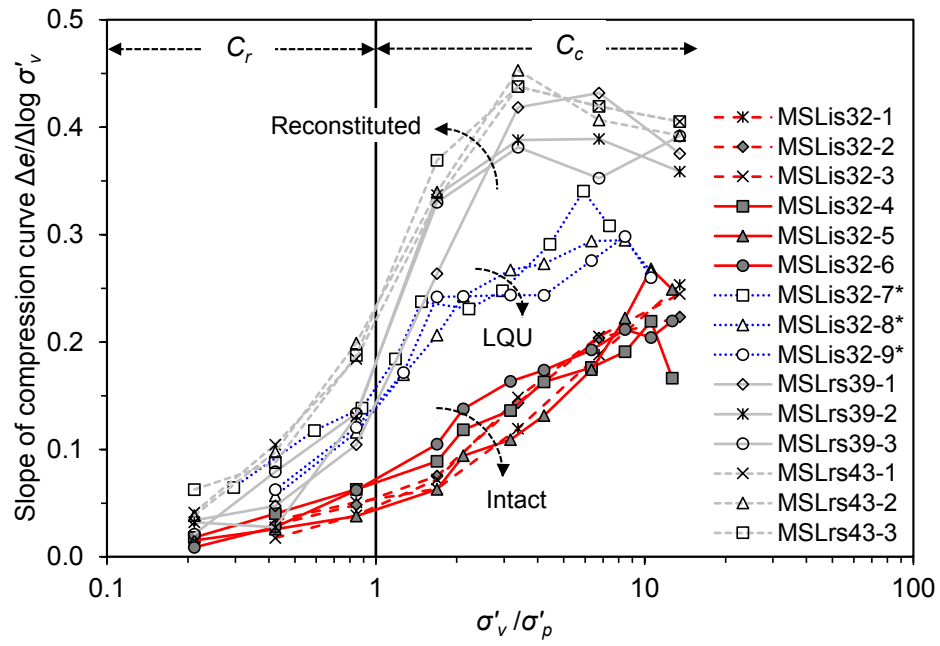


Fig. 9. Stress-dependency of the slope of compression curve for saturated intact, reconstituted, and LQU specimens

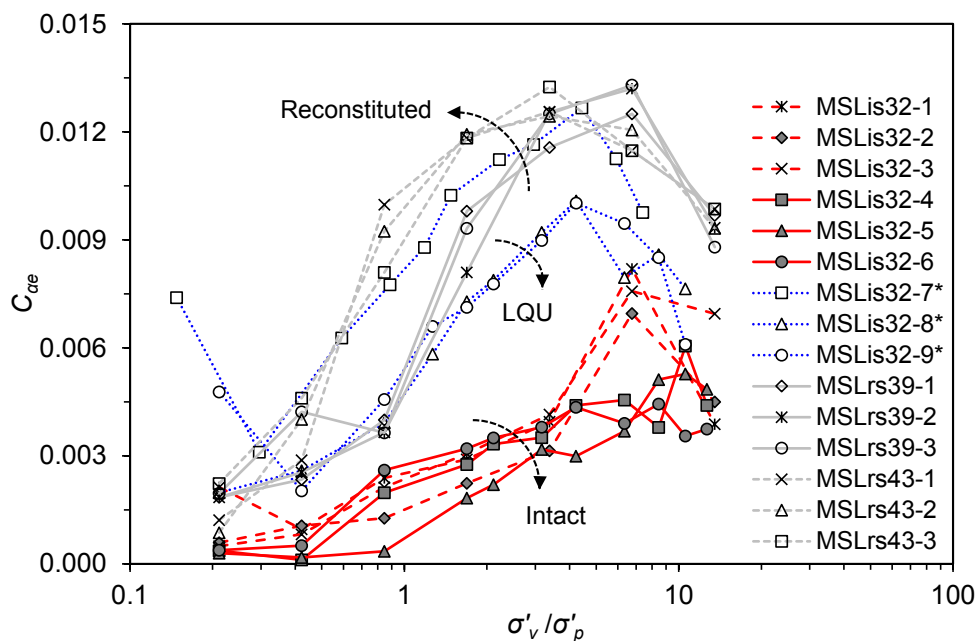


Fig. 10. Stress-dependency of C_{ae} for intact, reconstituted, and LQU specimens

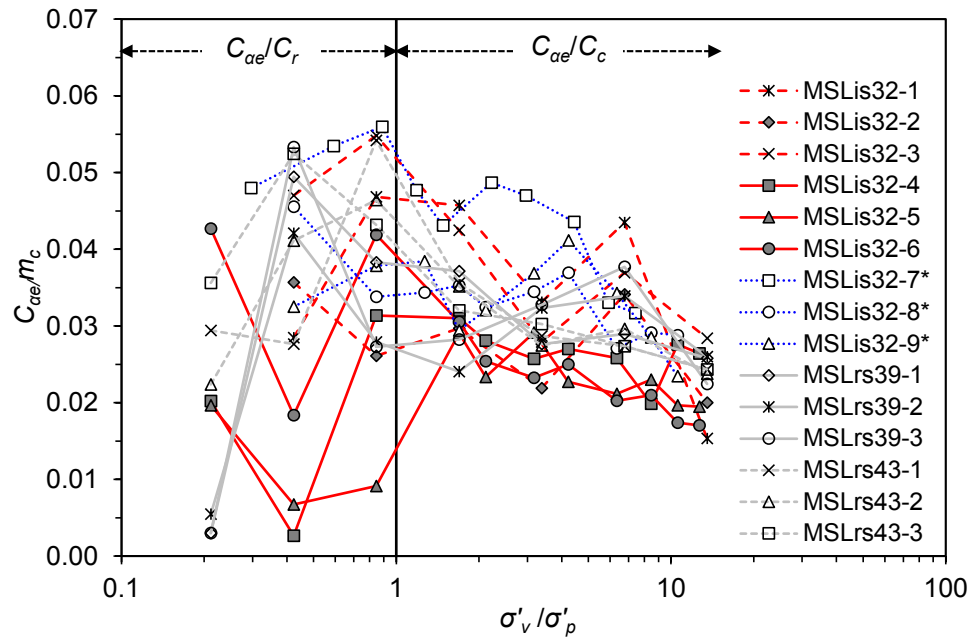


Fig. 11. Stress-dependency of C_{ae}/C_c for intact, reconstituted, and LQU specimens

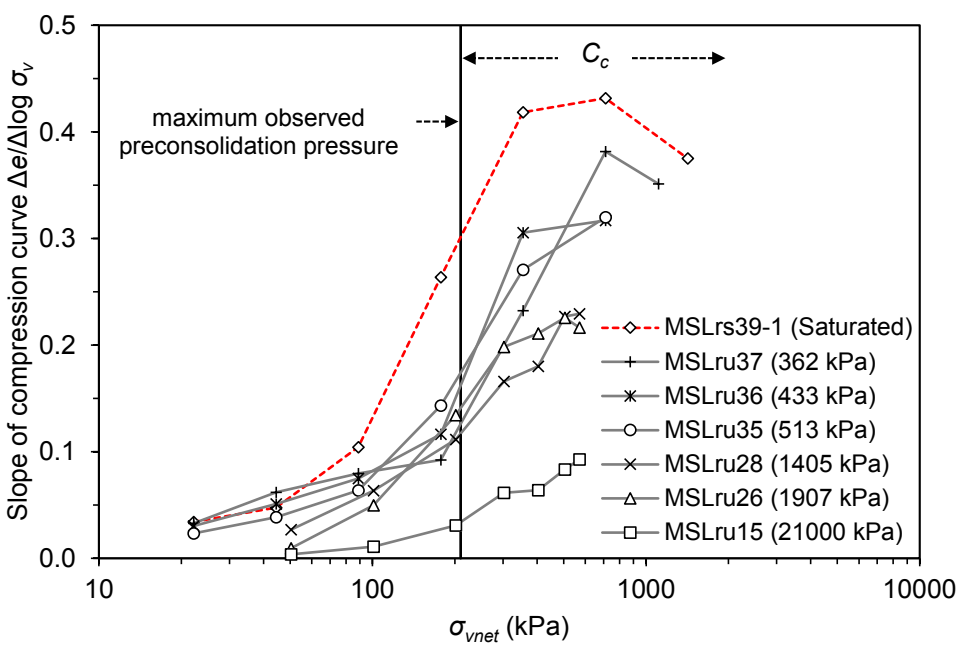


Fig. 12. Suction- and stress-dependency of the slope of compression curve for unsaturated reconstituted specimens

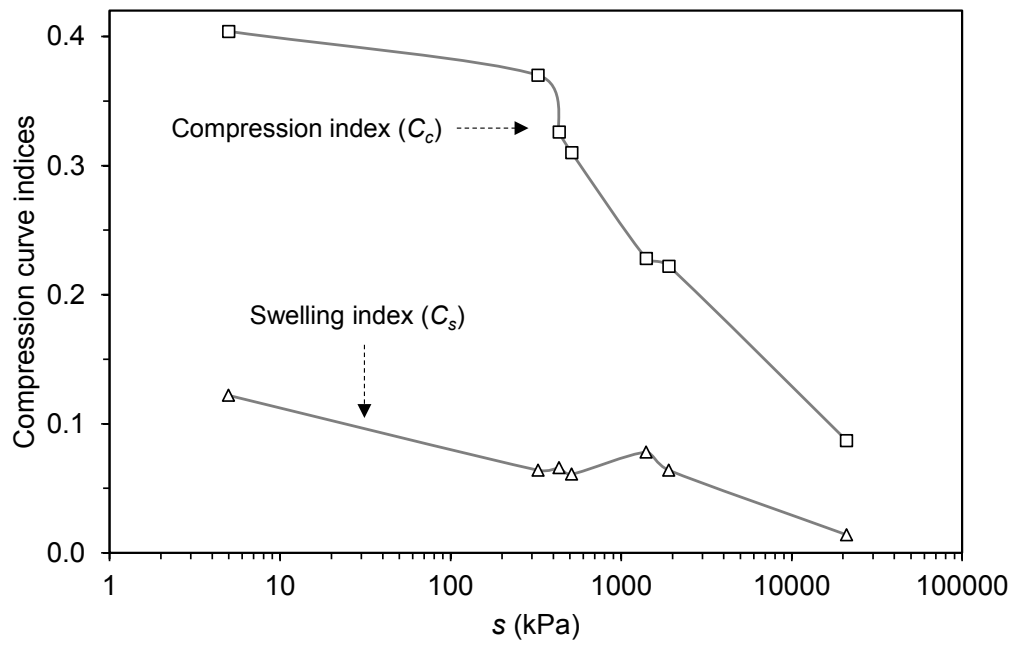


Fig. 13. Variation of C_c and C_s with suction for unsaturated reconstituted specimens

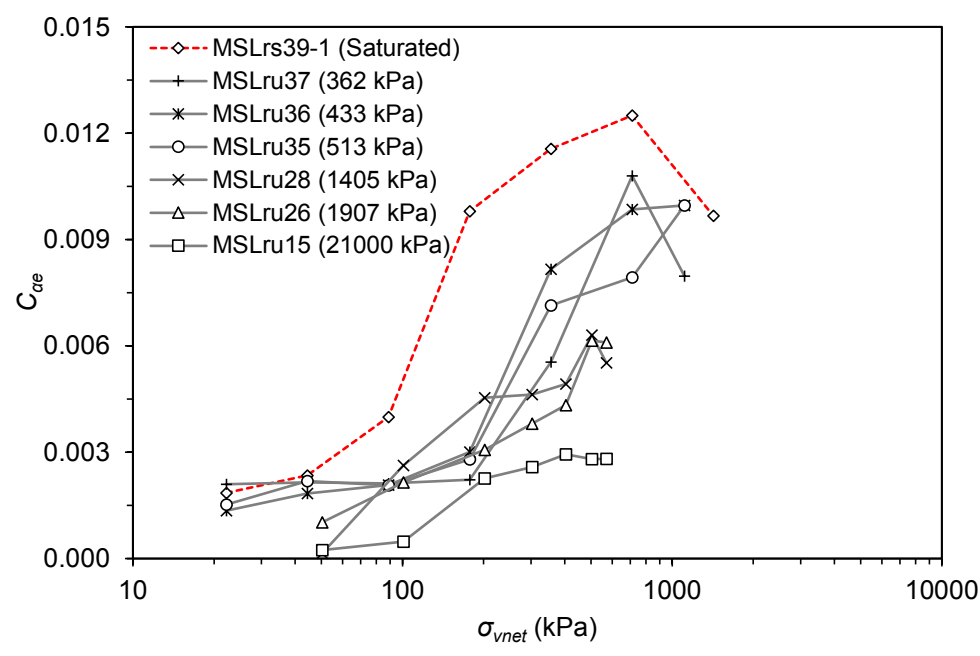


Fig. 14. Suction- and stress-dependency of C_{ae} for unsaturated reconstituted specimens

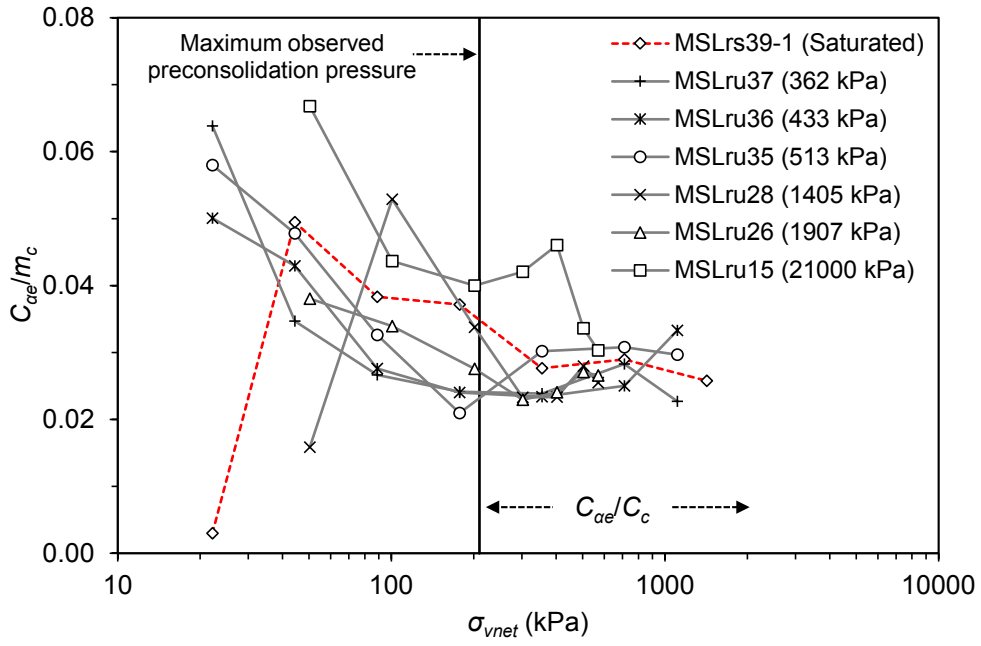


Fig. 15. Suction- and stress-dependency of the α ratio for unsaturated reconstituted specimens

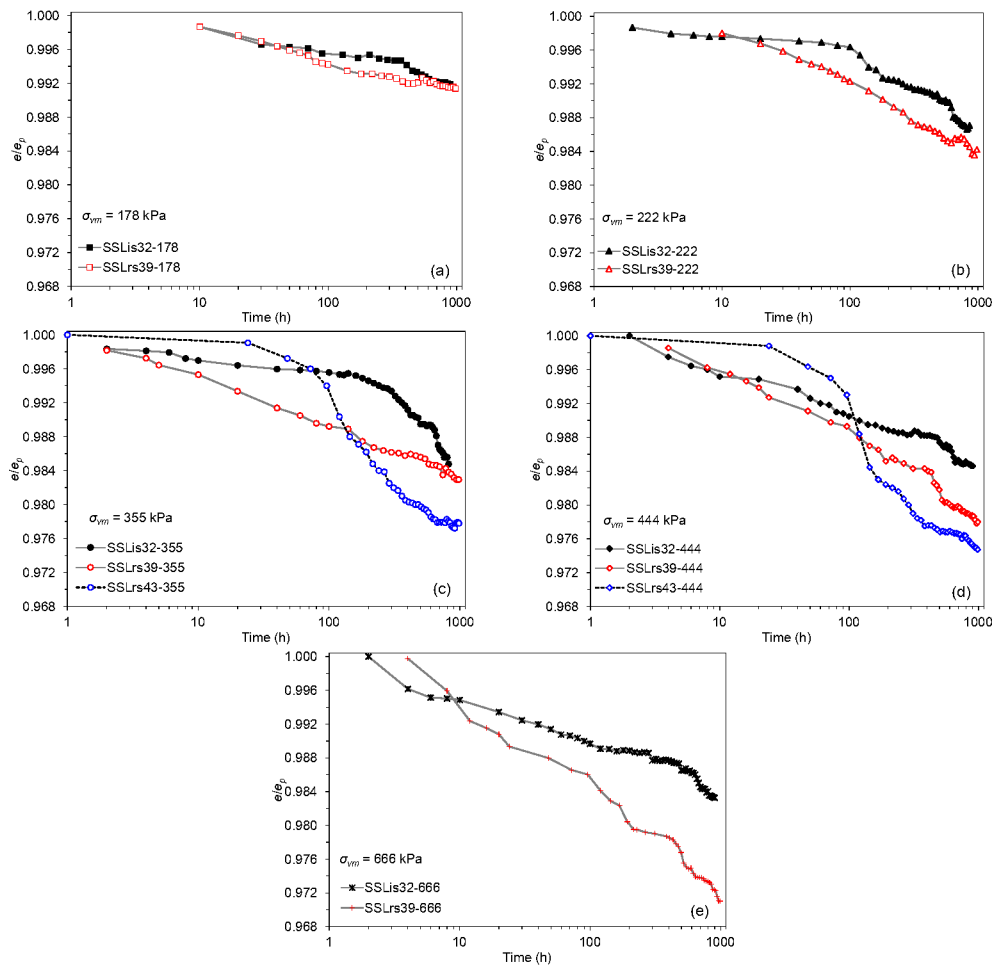


Fig. 16. SSL creep test results on intact and reconstituted specimens at stress levels of: (a) 178 kPa; (b) 222 kPa; (c) 355 kPa; (d) 444 kPa; (e) 666 kPa

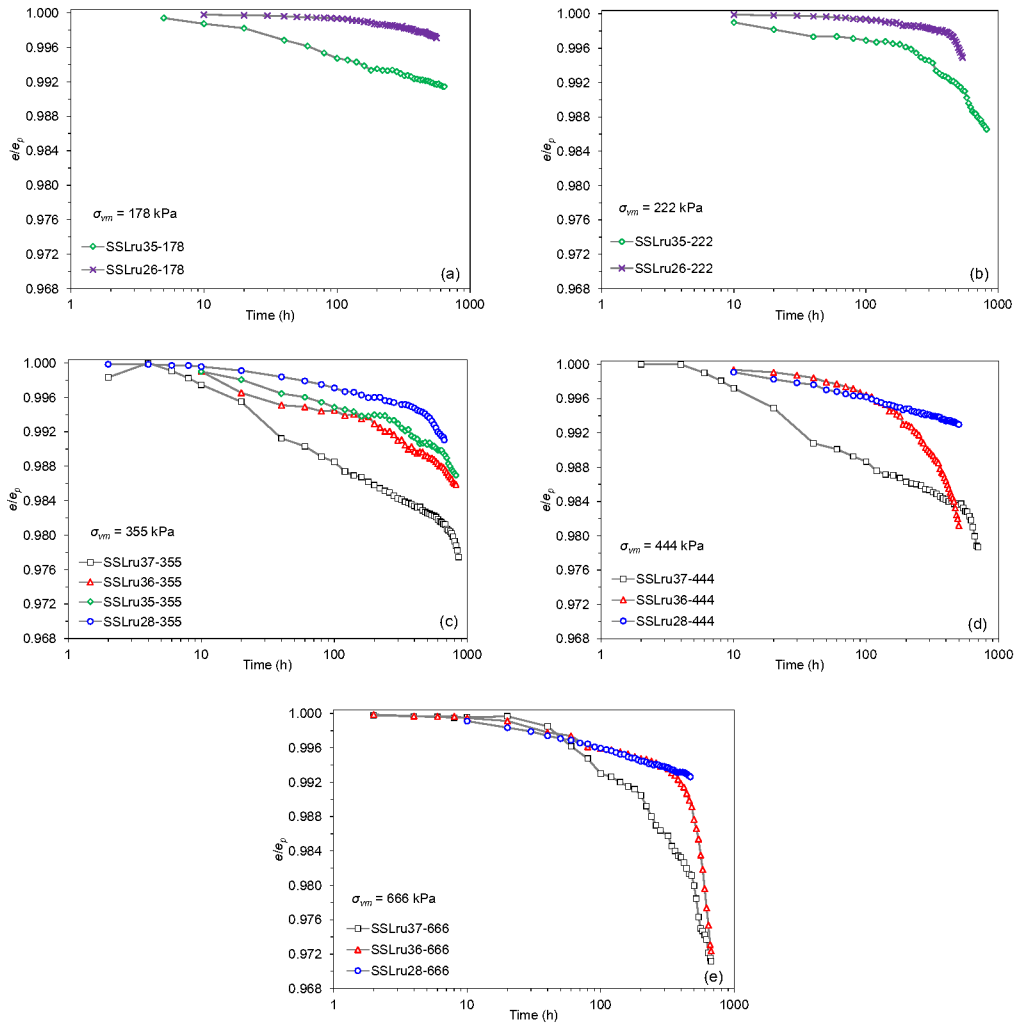


Fig. 17. SSL creep test results on unsaturated reconstituted specimens at stress levels of: (a) 178 kPa; (b) 222 kPa; (c) 355 kPa; (d) 444 kPa; (e) 666 kPa

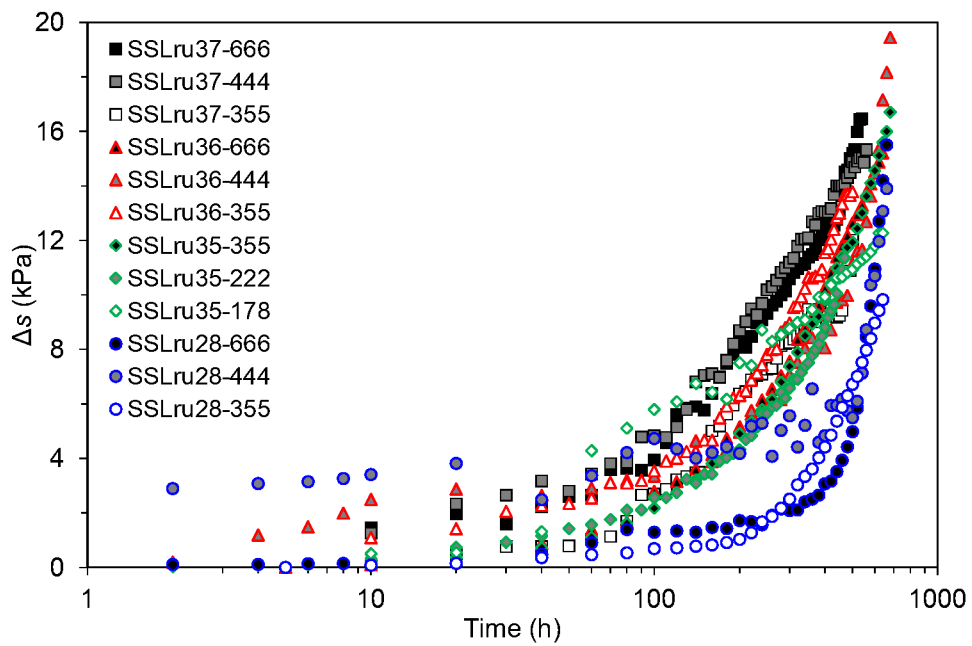


Fig. 18. Monitoring suction changes during creep stage of SSL oedometer tests